Reprinted from

Journal of volcanology and geothermal research

Journal of Volcanology and Geothermal Research 78 (1997) 1–29

Geochemistry vs. seismo-tectonics along the volcanic New Hebrides Central Chain (Southwest Pacific)

Michel Monzier [a,*], Claude Robin [a], Jean-Philippe Eissen [b], Jo Cotten [c]

[a] *ORSTOM, UR 1F, Apartado 17-11-6596, Quito, Ecuador*
[b] *ORSTOM, UR 1F, B.P. 70, 29280 Plouzané cedex, France*
[c] *URA 1278, Université de Bretagne Occidentale, B.P. 809, 29285 Brest, France*

ELSEVIER

Journal of volcanology and geothermal research

Scope of the journal

Papers covering the following aspects of volcanology and geothermal research will qualify for publication in the *Journal of Volcanology and Geothermal Research:* (1) geochemical aspects – geochemistry of volcanic rocks, geochemistry of volcanic gases and related products, isotope studies; (2) petrological aspects – magma genesis and magma evolution, petrology of volcanic rocks; (3) economic aspects – ore deposits related to volcanic rocks, geothermal energy; (4) geophysical aspects – physical properties of volcanic rocks and magmas, heat flow studies, physical volcanology, volcanic seismology, volcanic surveillance, geophysical exploration for geothermal resources; (5) tectonic aspects – relation of volcanism to global and regional tectonic processes; (6) environmental aspects – volcanic gases and their effect on the atmosphere.
Types of contribution to be published are: (1) research papers, (2) reviews, (3) short communications, (4) letters, (5) book reviews and (6) announcements.

Publication schedule and subscription information

Journal of Volcanology and Geothermal Research (ISSN 0377-0273). For 1997 volumes 75-80 are scheduled for publication. Subscription prices are available upon request from the publisher. Subscriptions are accepted on a prepaid basis only and are entered on a calendar year basis. Issues are sent by surface mail except to the following countries where air delivery via SAL is ensured: Argentina, Australia, Brazil, Canada, Hong Kong, India, Israel, Japan, Malaysia, Mexico, New Zealand, Pakistan, PR China, Singapore, South Africa, South Korea, Taiwan, Thailand, USA. For all other countries airmail rates are available upon request. Claims for missing issues must be made within six months of our publication (mailing) date. For orders, claims, product enquiries (no manuscript enquiries) please contact the Customer Support Department at the Regional Sales Office nearest to you:

New York, Elsevier Science, P.O. Box 945, New York, NY 10159-0945, USA. Tel: (+1) 212-633-3730, [Toll Free number for North American Customers: 1-888-4ES-INFO (437-4636)], Fax: (+1) 212-633-3680, E-mail: usinfo-f@elsevier.com

Amsterdam, Elsevier Science, P.O. Box 211, 1000 AE Amsterdam, The Netherlands. Tel: (+31) 20-485-3757, Fax: (+31) 20-485-3432, E-mail: nlinfo-f@elsevier.nl

Tokyo, Elsevier Science, 9-15, Higashi-Azabu 1-chome, Minato-ku, Tokyo 106, Japan. Tel: (+81) 3-5561-5033, Fax: (+81) 3-5561-5047, E-mail: kyf04035@niftyserve.or.jp

Singapore, Elsevier Science, No. 1 Temasek Avenue, #17-01 Millenia Tower, Singapore 039192. Tel: (+65) 434-3727, Fax: (+65) 337-2230, E-mail: asiainfo@elsevier.com.sg

(Text continued on inside back cover)

0377-0273/97/$17.00

PRINTED IN THE NETHERLANDS

ELSEVIER

Journal of Volcanology and Geothermal Research 78 (1997) 1–29

Journal of volcanology and geothermal research

Geochemistry vs. seismo-tectonics along the volcanic New Hebrides Central Chain (Southwest Pacific)

Michel Monzier [a,*], Claude Robin [a], Jean-Philippe Eissen [b], Jo Cotten [c]

[a] *ORSTOM, UR 1F, Apartado 17-11-6596, Quito, Ecuador*
[b] *ORSTOM, UR 1F, B.P. 70, 29280 Plouzané cedex, France*
[c] *URA 1278, Université de Bretagne Occidentale, B.P. 809, 29285 Brest, France*

Received 15 July 1996; accepted 3 January 1997

Abstract

Compositional variations (major- and trace-element) of Pleistocene to Present rocks along the volcanic New Hebrides Central Chain (Southwest Pacific) are presented and discussed, using a new set of analyses. We focus in particular on the anomalous Mg-, K-, LILE- and LREE-rich and Al- and Si-poor character of the basalts from Aoba and Santa Maria volcanoes (and, to a lesser extent, from Ambrym volcano), all located in the area where the D'Entrecasteaux Zone collides with the arc. In addition, we note a compositional transition from 'normal' arc basalts to boninite-related high-Mg andesites at the southern termination of the NHCC. The peculiar composition of the rocks of the volcanoes facing the D'Entrecasteaux Zone has traditionally been related, more or less directly, to the collision–subduction occurring in this area. We present an alternative hypothesis, of a strong geochemical anomaly under Santa Maria and Aoba volcanoes, unrelated to this collision. In this model, a westward and upward invasion of DUPAL-type enriched mantle, corroborated by the pattern of intermediate seismicity, occurs under this part of the arc, in strong contrast to the usual Pacific-type MORB mantle source present under all other volcanoes of the NHCC. Such a DUPAL-type source may explain the anomalous geochemistry of the resulting volcanic products.

Keywords: arc geochemistry; seismo-tectonics; along-arc variations; New Hebrides Central Chain; volcanic suites; enriched mantle; mantle sources

1. Introduction

In the Southwest Pacific, the New Hebrides arc overlies an E-dipping slab that corresponds to the subduction of the Australian plate under the North Fiji Basin (Fig. 1). This arc comprises four volcanic segments; the northernmost segment, essentially submarine and not well known, is not considered here. In this paper, the geochemical characteristics of the primitive magmas from the three volcanic segments forming the 1200-km-long New Hebrides Central Chain (NHCC) are discussed and related to the regional seismo-tectonic context. The NHCC stretches from Ureparapara island (Banks Islands) in the north, to Hunter island in the south (Fig. 2A). It comprises a Central Segment, a Southern Volcanic Segment (CVS and SVS) and a southernmost or High-Mg Andesite Volcanic Segment (HMAVS).

* Corresponding author. Fax: +593-2-569396; E-mail: monzier@orstom.ecx.ec

PII S0377-0273(97)00006-1

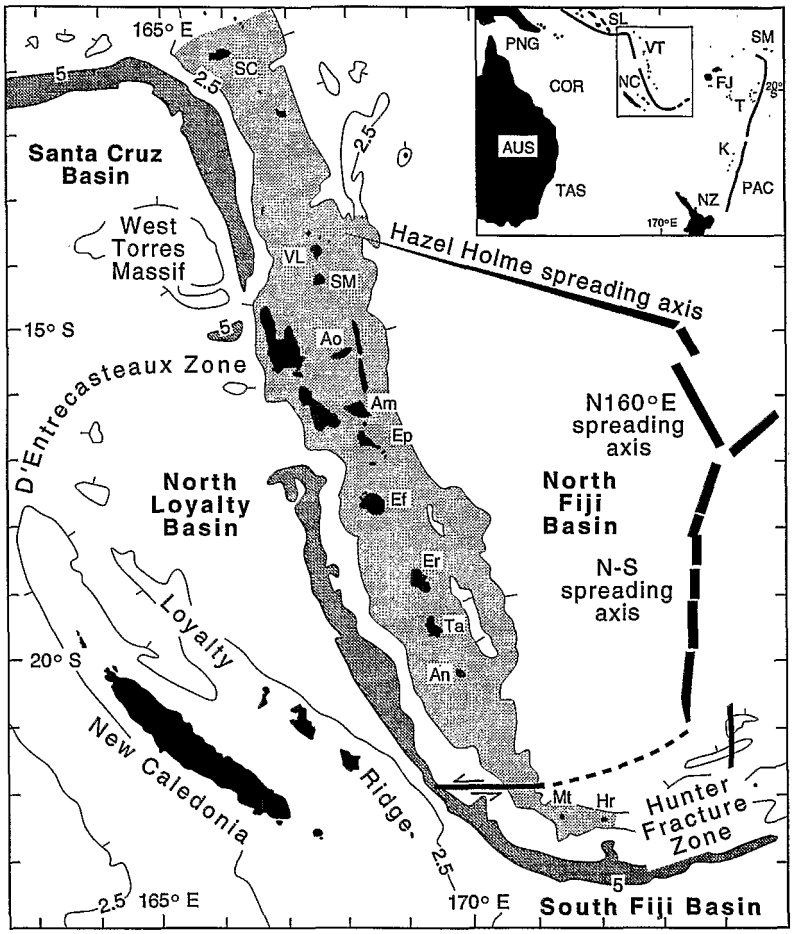

Fig. 1. Inset: The southwest Pacific. *AUS* = Australia; *PNG* = Papua New Guinea; *COR* = Coral Sea; *TAS* = Tasman Sea; *SL* = Solomon islands; *VT* = Vanuatu; *NC* = New Caledonia; *SM* = Samoa islands; *FJ* = Fiji islands; *T* = Tonga islands; *K* = Kermadec islands; *NZ* = New Zealand; *PAC* = Pacific Ocean. Large map: The New Hebrides trench (dark grey) and island arc (light grey). *SC* = Santa Cruz islands; *VL* = Vanua Lava island; *SM* = Santa Maria island; *Ao* = Aoba island; *Am* = Ambrym island; *Ep* = Epi island; *Ef* = Efate island; *Er* = Erromango island; *Ta* = Tanna island; *An* = Anatom island; *Mt* = Matthew island; *Hr* = Hunter island; North Fiji Basin spreading axes from Auzende et al. (1994) and Pelletier et al. (1993).

Most of the volcanic edifices are Pleistocene to Present in age. Late Miocene and Pliocene volcanics occur only on Erromango, Tanna and Anatom islands (Macfarlane et al., 1988).

2. Volcano-tectonic framework

2.1. The Central Volcanic Segment (CVS)

From Ureparapara to Kuwae, the CVS is slightly arcuate and convex towards the west (Fig. 2A). Its northern end includes the active Vanua Lava volcano and Ureparapara, a presently inactive, small volcano (Ash et al., 1980; Simkin et al., 1981). Morphotectonic characteristics of this part of the arc are quite usual; however, the West Torres Massif, on the Australian Plate, begins to enter the trench and the extensional back-arc area (Charvis and Pelletier, 1989; Recy et al., 1990) is complicated by the westwards propagation of the Hazel Holme spreading axis in the North Fiji Basin (Pelletier et al., 1993). The thickness of the crust ($\approx$ 14 km, Sage and Charvis, 1991) is typical of an intra-oceanic

island arc and both Vanua Lava and Ureparapara volcanoes show 'normal' island arc magmatic suites (i.e., low-K, Macfarlane et al., 1988). Mere Lava active volcano, which is clearly off-axis relative to the NHCC, is not considered in this study.

The central part of the CVS comprises three large

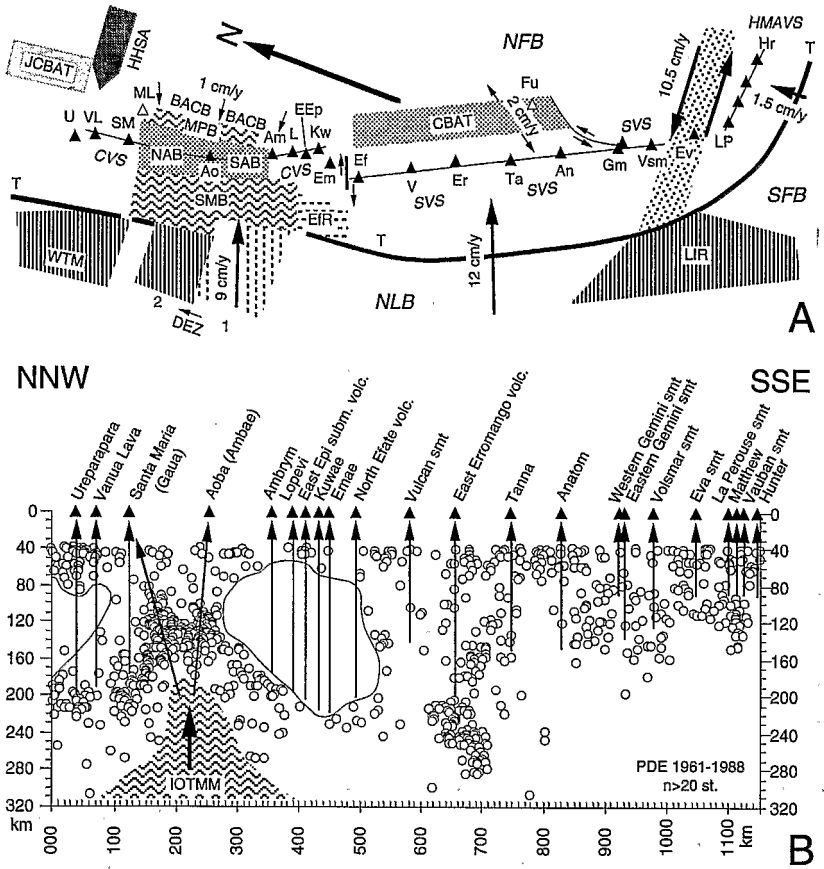

Fig. 2. (A) Schematic map of the New Hebrides island arc. Australian Plate: *WTM* = West Torres Massif; *DEZ* = D'Entrecasteaux Zone (the small arrow and positions *1* and *2* approximatively indicate the northward migration of the *DEZ* along the arc during the last 2 or 3 m.y. due to their obliquity in relation to the convergence direction); *NLB* = North Loyalty Basin; *LIR* = Loyalty Islands Ridge; *SFB* = South Fiji Basin; *T* = deep trench (depth > 6 km). New Hebrides island arc: *SMB* = Santo-Mallicolo block; *EfR* = Efate Reentrant; *CVS* = Central Volcanic Segment; *U* = Ureparapara island; *VL* = Vanua Lava island; *SM* = Santa Maria island; *NAB* = North Aoba Basin; *Ao* = Aoba island; *SAB* = South Aoba Basin; *Am* = Ambrym island; *L* = Lopevi island; *EEp* = East Epi seamounts; *Kw* = Kuwae caldera; *Em* = Emae island; *SVS* = Southern Volcanic Segment; *Ef* = Efate island; *V* = Vulcan seamount; *Er* = Erromango island; *Ta* = Tanna island; *An* = Anatom island; *Gm* = Gemini seamounts; *Vsm* = Volsmar seamount; *Ev* = Eva seamount; *HMAVS* = High-Mg Andesites Volcanic Segment; *LP* = La Pérouse seamount; *Hr* = Hunter island; *JCBAT* = Jean Charcot Back-Arc Troughs; *HHSA* = Hazel Holme Spreading Axis; *ML* = Mere Lava island; *MPB* = Maewo-Pentecost Block; *BACB* = Back-Arc Compressive Belt; *CBA* = Coriolis Back-Arc troughs; *Fu* = Futuna island. NFB = North Fiji Basin. Convergence rate at the NH trench, senestral motion along the E–W boundary intersecting the arc in front of the *LIR* and compressive or distensive motions in the back-arc area (all in cm/yr) from Louat and Pelletier (1989). (B) Along-arc (N160°E) vertical projection of the 1961–1988 shallow and intermediate seismicity, at the same scale as A (USGS–NEIC, 1961–1988). Only the seisms recorded by more than 20 stations are used; a heavy line under each volcanoes (▲) approximatively represents the probable magma path (see Fig. 3 and text for the Garet–Santa Maria case). The main gaps of seismicity are enhanced. The upward and westward propagation of a deep regional body of Indian Ocean-type MORB mantle (IOTMM) under Santa Maria and Aoba islands is also represented (see text and Fig. 3Fig. 9).

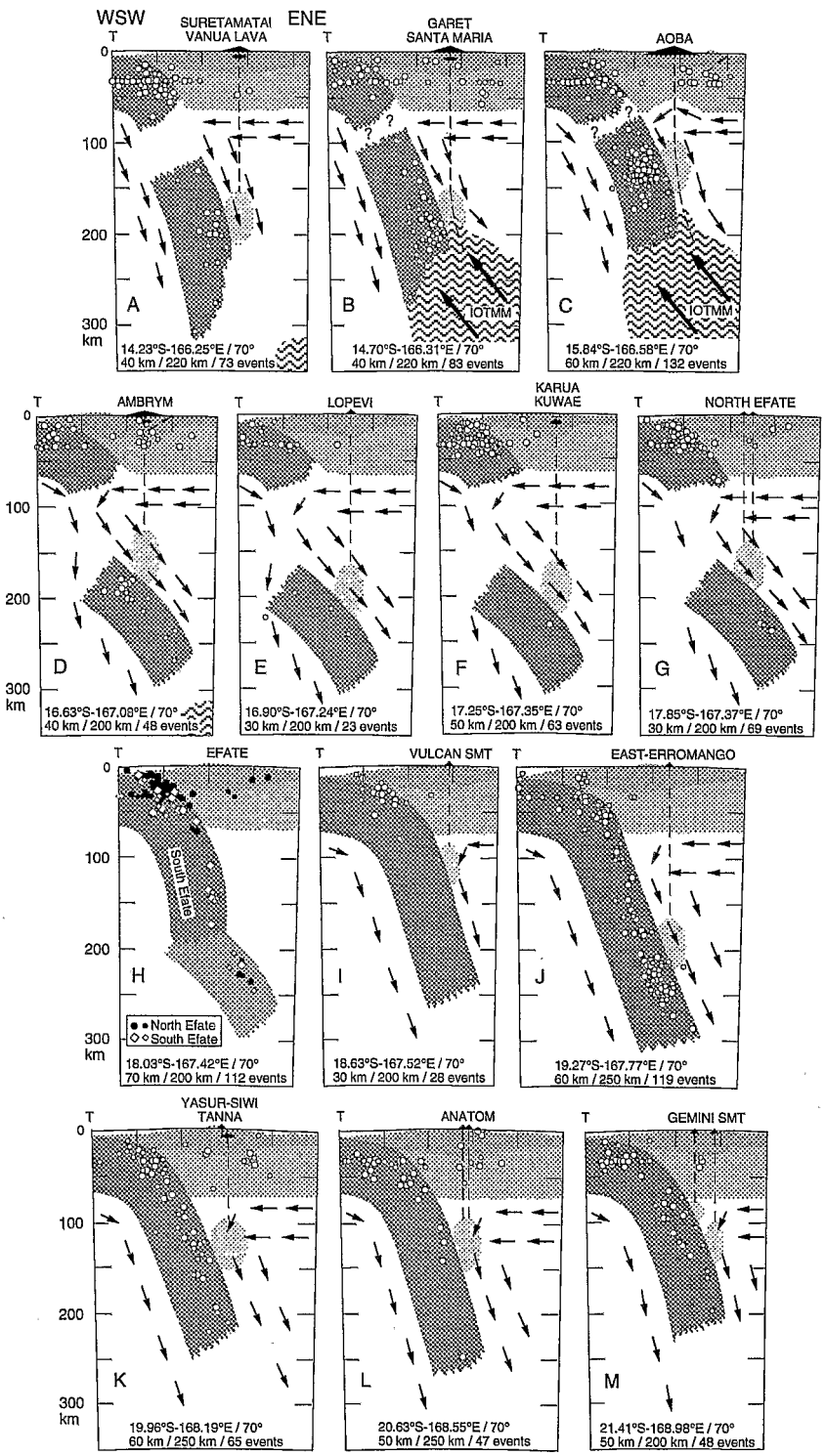
WSW
ENE
SURETAMATAI
VANUA LAVA
GARET
SANTA MARIA
AOBA
T
0
100
200
300
km
A
B
C
IOTMM
14.23°S-166.25°E / 70°
40 km / 220 km / 73 events
14.70°S-166.31°E / 70°
40 km / 220 km / 83 events
15.84°S-166.58°E / 70°
60 km / 220 km / 132 events
AMBRYM
LOPEVI
KARUA
KUWAE
NORTH EFATE
D
E
F
G
16.63°S-167.08°E / 70°
40 km / 200 km / 48 events
16.90°S-167.24°E / 70°
30 km / 200 km / 23 events
17.25°S-167.35°E / 70°
50 km / 200 km / 63 events
17.85°S-167.37°E / 70°
30 km / 200 km / 69 events
EFATE
VULCAN SMT
EAST-ERROMANGO
South Efate
H
I
J
North Efate
South Efate
18.03°S-167.42°E / 70°
70 km / 200 km / 112 events
18.63°S-167.52°E / 70°
30 km / 200 km / 28 events
19.27°S-167.77°E / 70°
60 km / 250 km / 119 events
YASUR-SIWI
TANNA
ANATOM
GEMINI SMT
K
L
M
19.96°S-168.19°E / 70°
60 km / 250 km / 65 events
20.63°S-168.55°E / 70°
50 km / 250 km / 47 events
21.41°S-168.98°E / 70°
50 km / 200 km / 48 events

active volcanoes. Aoba volcano is built at the centre of the Aoba Basin, and divides it into two parts, the North Aoba Basin and the South Aoba Basin. This volcano is mainly basaltic (Warden, 1970; Eggins, 1989), whereas Santa Maria and Ambrym, located at the extremities of the Aoba Basin, consist of basalts and subordinate differentiated rocks (Mallick and Ash, 1975; Robin et al., 1993, 1995; Picard et al., 1995). Since ≈ 2–3 Ma, the structural evolution of this area has been controlled by the collision between the D'Entrecasteaux Zone (DEZ), a twin E–W-oriented ridge system rising 2 to 4 km above the abyssal plain of the Australian Plate, and the arc (Maillet et al., 1983; Collot et al., 1985, 1992; Burne et al., 1988; Greene and Collot, 1994; Taylor et al., 1994). As a result of this collision, plate coupling is strong and the convergence rate is relatively low at the trench (9 cm/yr on average, from Louat and Pelletier, 1989; only 3.6 cm/yr for the 1990–1994 period, from Calmant et al., 1995). Additionally, shortening occurs in the back-arc area, where the North Fiji Basin underthrusts the Maewo–Pentecost block at a rate of ≈ 1 cm/yr (Collot et al., 1985; Louat and Pelletier, 1989).

The North Aoba Basin appears as a broad flexural depression between the uplifted Santo-Mallicolo and Maewo–Pentecost blocks (Collot et al., 1985; Greene et al., 1994). Its thin crust comprises a 4-km-thick volcano-sedimentary fill which includes an intermediate volcanic sill, overlying a typical 7.5–8.5-km-thick oceanic crust (Pontoise et al., 1994). The South Aoba Basin is shallower and probably has a distinct and more fractured crust than the North Aoba Basin (B. Pontoise, pers. commun.). Transverse fracture zones, which tend to open under the compressive stresses related to the DEZ collision, provide an easy pathway for the ascent of magmas under Aoba and Ambrym (and Santa Maria?) volcanoes. Thus, the great fracture zone of Aoba, located at the boundary between two crustally distinct basins, plus the thinness of the North Aoba Basin crust, would partially explain the particulary mafic nature and the high lava production rate of this volcano, by far the most voluminous volcano of the NHCC (≈ 2500 km^3; Ambrym, second in size, has only a volume of ≈ 500 km^3). Interestingly, this high lava production rate correlates with little or no island arc plutonism within or under the crust underlying Aoba island (Pontoise et al., 1994). High K, LILE and LREE contents in rocks from Santa Maria, Aoba and Ambrym volcanoes have always been related, more or less directly, to the DEZ collision–subduction (Gorton, 1974, 1977; Roca, 1978; Girod et al., 1979; Barsdell et al., 1982; Dupuy et al., 1982; Crawford et al., 1988; Macfarlane et al., 1988; Eggins, 1989, 1993; Hasenaka et al., 1994). We discuss this topic in more detail below.

The southern end of the CVS is very active, though volcanic edifices are not volumetrically important. From north to south, this part of the arc includes the Lopevi active volcano (Warden, 1967), three active submarine volcanoes near Epi island (Crawford et al., 1988) and the Karua active submarine volcano in the 500 year old Kuwae caldera

Fig. 3. Transverse (N70°E) WSW–ENE cross sections beneath the volcanoes of the Central and Southern Volcanic Segments (no vertical exageration). T = Trench. As for Fig. 2B, only the earthquakes recorded by more than 20 stations are used (USGS–NEIC, 1961–1988). Larger symbols correspond to seisms with $M = 5–7$ whereas smaller ones correspond to seisms with $M < 5$. Parameters shown at the base of each cross section are: latitude and longitude of the point of the trench at the origin (km 0) of the axis of the section/orientation of this axis/width of the stripe projected on the section in km (half width on each side of the axis)/along-axis length of the section/number of events. North and South Efate data have been reported with different symbols on the Efate section (this wide Efate section including the narrow North Efate section). Schematic interpretation of the sinking Australian Plate lithosphere and its detached parts as well as approximative thickness for the New Hebrides arc crust and lithosphere after data discussed in the text. Magma path is shown by a dashed line on each section. Deduced flows in the upper mantle are schematically drawn. The upward and westward propagation of a deep regional body of Indian Ocean-type MORB mantle (IOTMM) under Santa Maria and Aoba islands is also shown (see text and Fig. 2Fig. 9). Intra-crustal volcanic chambers are represented beneath some volcanic edifices with large and recent calderas. Westward dipping reverse faulting (back-arc compressive belt) is shown on Aoba and Ambrym sections. Aoba is, by far, the most voluminous of all the volcanoes of the NHCC, which implies, in physical terms, a greater thermal imput than for the other volcanoes (Mitropoulos and Tarney, 1992). The crust is unusually thin under this volcano (see text), but in addition, and as a possible response to this high thermal release, lithosphere thinning is also represented beneath it.

(Monzier et al., 1994; Robin et al., 1994b). Recently extinct volcanic cones are also present on Epi, Tongoa and Emae (Warden et al., 1972). Here, the thickness of the crust is not known, but is probably similar to that of the northern end of the CVS (i.e., ≈ 15 km) and the fore-arc slope shows a wide reentrant, the Efate reentrant, a consequence of the early subduction of the DEZ under the arc (Greene and Collot, 1994), or of the subduction of large seamounts (Collot and Fisher, 1989). Geochemical characteristics of the southern CVS volcanoes are generally 'normal' (i.e., low-K, Macfarlane et al., 1988). The boundary between the CVS and the SVS occurs between Kuwae and Efate volcanoes and appears as a sharp dextral jump, where the Emae volcanoes are located.

2.2. The Southern Volcanic Segment (SVS)

The rectilinear SVS (Fig. 2A), often considered as the 'normal' part of the arc, is characterized, at least from Efate to Anatom, by large uplifted islands, formed by coalescent volcanoes (Colley and Ash, 1971; Ash et al., 1978; Carney and Macfarlane, 1979; Coulon et al., 1979; Coulon and Maury, 1981; Marcelot, 1980, 1981; Marcelot et al., 1983; Robin et al., 1994a). South of Anatom, the SVS becomes entirely submarine and the size of the edifices decreases (Monzier et al., 1984a, 1992). As noted by Greene et al. (1988), a remarkable feature of this segment is the almost constant volcano spacing (≈ 90 km). Historic submarine activity has been reported east of Erromango, whereas Yasur volcano in Tanna has been constantly active since its discovery by Cook in 1774 (Simkin et al., 1981). In February 1996, the Eastern Gemini Seamount erupted, but no other information exists about the activity of the submarine volcanoes of the SVS.

Morpho-tectonic characteristics of the SVS include a deep trench, a large arc ridge, the size of which decreases south of Anatom, and an active extension zone at the Coriolis back-arc troughs (Louat and Pelletier, 1989; Recy et al., 1990). Convergence rate at the trench is higher than that at the CVS. In front of Tanna, Louat and Pelletier (1989) give a rate of 12 cm/yr, a value subsequently confirmed by geodetic measurements (GPS observations) during the 1990–1994 period (11.7 cm/yr; Calmant et al., 1995). The SVS lies on a crust which is thicker than the CVS crust (≈ 25–30 km; Ibrahim et al., 1980; Pontoise et al., 1980; Coudert et al., 1984). Geochemical characteristics of the SVS suites are those of a low-K 'normal' intra-oceanic island arc (Macfarlane et al., 1988). Futuna island, clearly off-axis relative to the NHCC, is not considered here.

2.3. The High-Mg Andesite Volcanic Segment (HMAVS)

The boundary between the SVS and the HMAVS occurs near the Eva seamount (22°S), in front of the collision zone between the Loyalty Islands Ridge (on the Australian plate) and the arc. Though quite recent, this collision strongly influenced the structural configuration of the southern trench and arc, best demonstrated by the 10.5 cm/yr E–W-trending sinistral transform fault which forms a new plate boundary in front of the Loyalty salient (Louat and Pelletier, 1989; Monzier et al., 1990, 1993; Monzier, 1993). This collision probably explains both the decreasing size of the arc ridge and the disappearance of the Coriolis troughs south of Anatom.

All the volcanic edifices of the E–W-trending HMAVS (Fig. 2A) are of small volume (20–120 km^3), with the exception of Vauban Seamount (240 km^3) (Monzier et al., 1992, 1993). Most edifices are wholly submarine, but Matthew and Hunter volcanoes emerge, forming small islands where recent volcanic activity has been reported (Maillet et al., 1986). The subduction under this southernmost segment of the arc has a northward trend and is very low (about 1.5 cm/yr, according to Louat and Pelletier, 1989).

A high-Mg andesite suite, whose mafic endmembers are closely related to high-Ca boninites, characterizes the HMAVS. Southward propagation of the N–S-oriented active spreading axis of the North Fiji Basin into the arc probably accounts for a high thermal regime in this area and for the generation of high-Ca boninites by melting of a refractory hydrated mantle at shallow depth. Subsequent fractional crystallization and magma mixing processes produce the high-Mg andesite suite (Crawford et al., 1989, 1993; Monzier et al., 1993; Sigurdsson et al., 1993).

3. Seismological constraints

A projection of the shallow and intermediate seismicity (1961–1988) along the arc is shown in Fig. 2B, with inferred slab-to-volcanoes pathways (see also Fig. 3). A strikingly unusual feature is the archlike outline of the intermediate event distribution beneath Santa Maria and Aoba volcanoes, first observed by Blot (1972). At each side of this arch, two seismic gaps occur, the larger extends beneath Ambrym to Efate volcanoes (see Fig. 3D–G). Marthelot et al. (1985) have shown that a zone of attenuation of the high-frequency shear waves overlaps this large gap. In the same area, a shallow double seismic zone

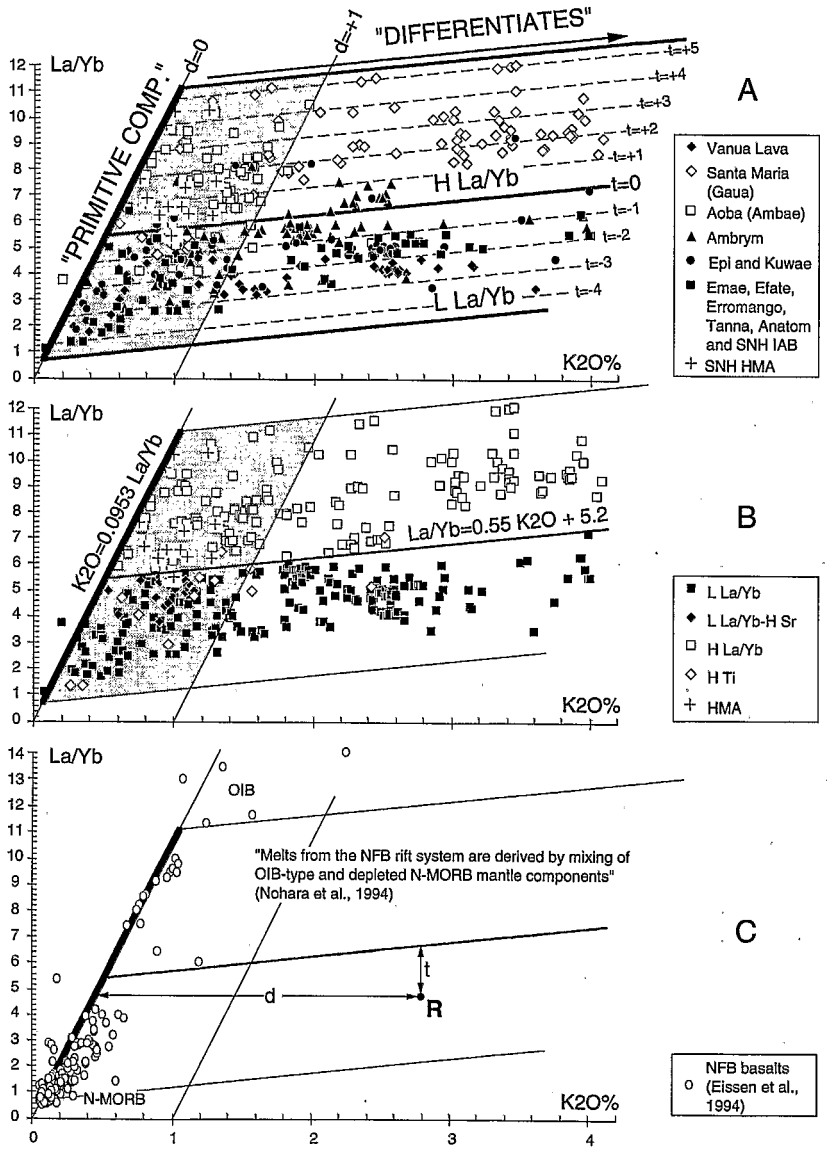

Fig. 4. (A) La/Yb vs. K_2O% diagram for NHCC compositions; the shaded area represents the primitive compositions set used to average calculations (Table 1Table 2) and in Fig. 6Fig. 7Fig. 8. (B) Classification proposed in this publication (see text). (C) La/Yb vs. K_2O% diagram for basalts from the North Fiji Basin spreading axes (all data LOI free and normalized to 100%).

occurs near the trench. All these observations are interpretated by Chatelain et al. (1992, 1993) and Prévot et al. (1994) in terms of slab detachment within the last 1 m.y. and resistance to subduction of the short remaining piece of Australian lithosphere.

Another unusual feature is the sharp shortening of the slab south of Anatom island, which has been related by Louat et al. (1988) to a southwards propagation of the subduction, but more recently considered by Monzier (1993) as an effect of the ongoing Loyalty Islands Ridge vs. New Hebrides arc collision.

Schematic sections across the CVS and SVS subduction zones are shown in Fig. 3. Though schematic, these sections underline some constraints for the geometry of the slab and the asthenospheric mantle wedge beneath the arc. They illustrate well the detached part of the slab sinking beneath volcanoes from Ambrym to Efate, with an ENE dip of about 50°, and the very short upper piece of dipping Australian lithosphere which remains in this zone (Fig. 3D–G). Here, the mantle wedge appears more narrow, than under the 'normal' part of the arc, where the subduction pattern shows an unbroken 70° dipping slab (Fig. 3I–M). In addition, interactions between the Australian and North Fiji Basin asthenospheric mantle flow regimes might occur through the slab window.

In the northern part of the CVS, beneath Vanua Lava, Santa Maria and Aoba volcanoes (Fig. 3A–C), the subduction pattern appears quite 'normal', with a 70–80° ENE-dipping slab. Slab detachment is probably occurring beneath Santa Maria and Aoba islands, but this phenomenon is obviously more recent (or slower) than beneath Ureparapara–Vanua Lava to the north, and Ambrym to North Efate to the south.

4. Geochemical data

4.1. Data file

This study includes previous published analyses as well as recently published and unpublished analyses carried out during the 1989–1994 ORSTOM program of volcanology in Vanuatu (whose targets were: Vanua Lava, Santa Maria, Aoba, Ambrym, Kuwae, Tanna and the southernmost NHCC). Only analyses with trace-element data (including La and Yb contents) have been retained, except for Ureparapara, Lopevi and Vulcan basalts, for which no analysis with such characteristics is available, but which are important for discussing the along-arc basalt geochemical variations. For normalization purposes, all major-element data (wt.%) have been recalculated to 100%, loss of ignition (LOI) and volatiles free, with total iron as $Fe_2O_3^*$ ($= Fe_2O_3 + 1.11FeO$). The data file (Microsoft Excel 4.0) comprises 404 major- and trace-element analyses, 334 of which (i.e., 83%) are from the ORSTOM volcanological program [analytical techniques, limits of detection and relative standard deviations for these 334 analyses are detailed in Monzier et al. (1993) and Picard et al. (1995)].

References for the source chemical data are:

Ureparapara: Ash et al., 1980; Barsdell et al., 1982; Monjaret, 1989.
Vanua Lava: ORSTOM unpublished data.
Santa Maria (Gaua): Barsdell et al., 1982; ORSTOM unpublished data.
Aoba (Ambae): Gorton, 1977; Eggins, 1989; ORSTOM unpublished data.
Ambrym: Gorton, 1977; Picard et al., 1995.
Lopevi: Warden, 1967.
West and East Epi: Gorton, 1977; Dupuy et al., 1982; Barsdell and Berry, 1990.
Epi A, B submarine volcanoes: Crawford et al., 1988.
Kuwae (including the easternmost part of Epi island, Ririna and Laika islets, Karua submarine volcano and Tongoa island): Gorton, 1977; Dupuy et al., 1982; Crawford et al., 1988; ORSTOM unpublished data.
Emae: Dupuy et al., 1982.
Efate (including Nguna, Pele, Emau and Mataso islands): Dupuy et al., 1982.
Vulcan seamount: Vallot, 1984.

Fig. 5. (a) Selected major- and trace-element diagrams for the NHCC rocks (all data LOI free and normalized to 100%). (b) Selected major- and trace-element diagrams for the NHCC rocks (all data LOI free and normalized to 100%).

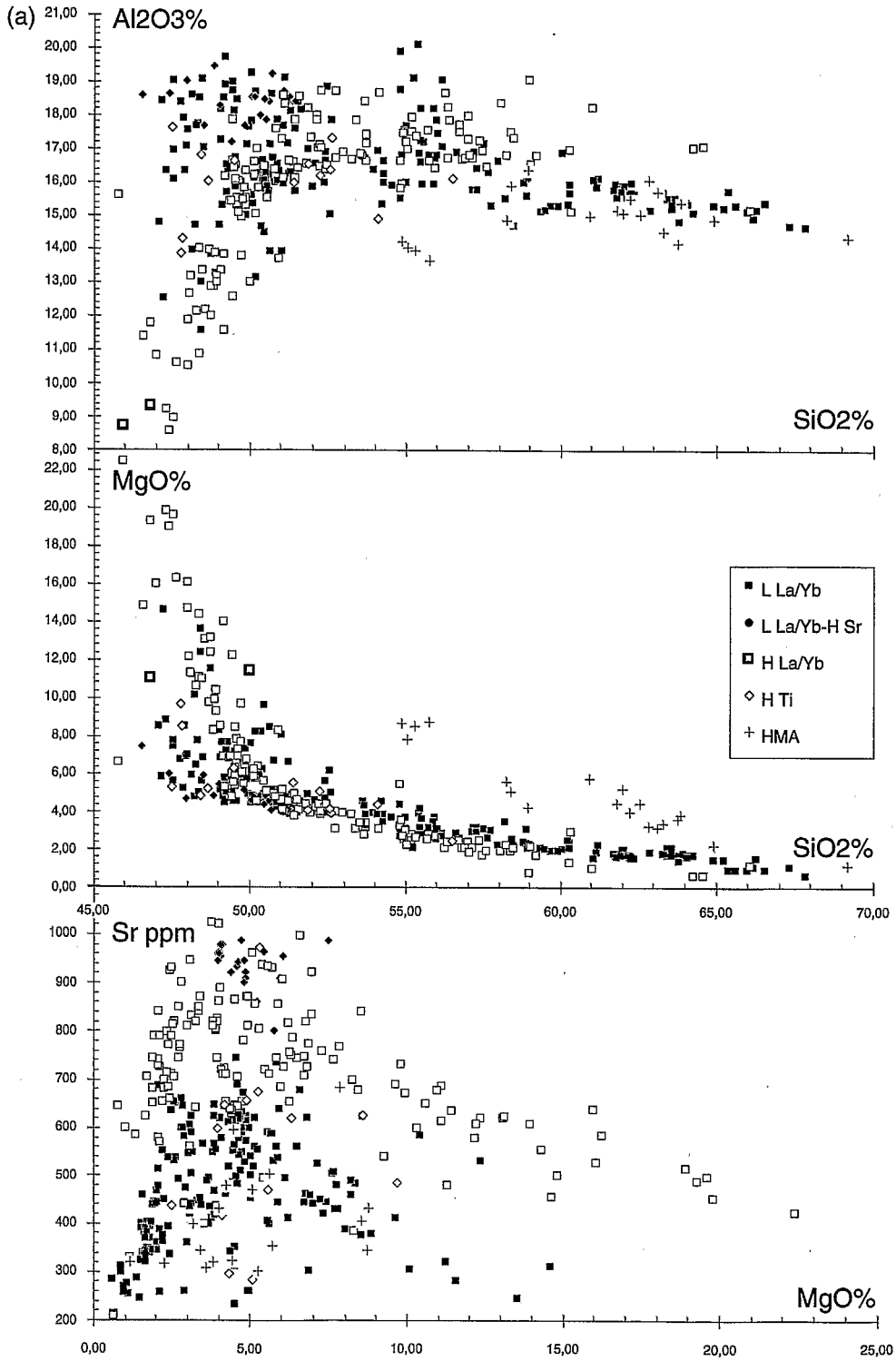
(a)
Al2O3%
SiO2%
MgO%
SiO2%
L La/Yb
L La/Yb-H Sr
H La/Yb
H Ti
HMA
Sr ppm
MgO%

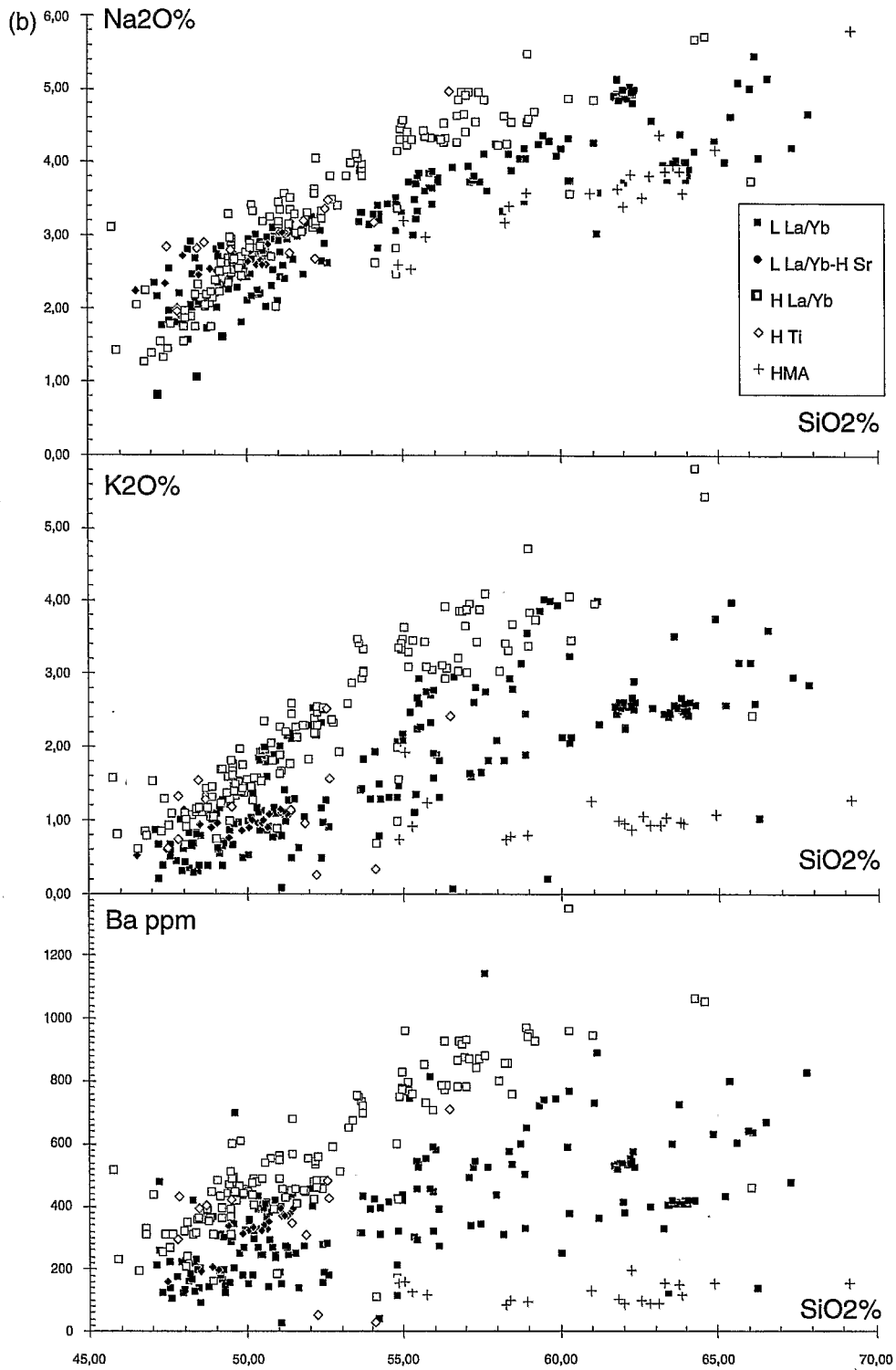

Fig. 5 (continued).

Erromango: Marcelot, 1981; Dupuy et al., 1982.
Tanna: Dupuy et al., 1982; Robin et al., 1994a; ORSTOM unpublished data.
Anatom: Dupuy et al., 1982.
Southernmost NHCC (from Gemini seamounts to Hunter): Monzier et al., 1993.

Following Gill (1981), in this study basalts are rocks with a SiO_2 content $< 53\%$ (recalculated on an anhydrous basis), andesites are subdivided into basic andesites (53–57% SiO_2) and acid andesites (57–63% SiO_2), and dacites range from 63 to 70% SiO_2.

4.2. La/Yb vs. K_2O systematics

The K_2O vs. SiO_2 diagram has been widely used to present individual suites or to discuss the general geochemistry of the arc (Macfarlane et al., 1988). However, on this diagram, basaltic compositions of individual suites tend to merge, making discrimination of primitive compositions difficult. For classification and discussion of the NHCC volcanic suites, we propose the La/Yb vs. K_2O process identification diagram, which better discriminates the different suites and the corresponding primitive compositions. On this diagram, compositions delineate gently rising parallel trends characterized by the equation '$La/Yb = 0.55\,K_2O$' (Fig. 4A). Obviously, the La/Yb value prevails for the discrimination between the different suites whereas the K_2O content more effectively shows differentiation. As a first observation, differentiated rocks are better represented than in previous study by Macfarlane et al. (1988), a probable consequence of the emphasis put on analysis of pyroclastic products during the ORSTOM volcanological program. A straight line through the origin, whose equation is '$K_2O = 0.0953\,La/Yb$' (Fig. 4B), may be considered as the primitive trend for NHCC rocks, since almost all compositions plot to the right of this line. Interestingly, most North Fiji Basin basalt compositions (Eissen et al., 1994; Nohara et al., 1994) also plot close to and to the right of this line (Fig. 4C).

Though a continuous compositional spectrum exists, for simplification purposes, the field defined by the NHCC rocks on this diagram has been divided by a line whose equation is '$La/Yb = 0.55\,K_2O + 5.2$', which separates high-La/Yb (HLa/Yb) compositions from those with low La/Yb (LLa/Yb) (Fig. 4B). Parameters t and d (Fig. 4C) characterize each composition reported on the diagram; t corresponds to the La/Yb value in relation to the previously defined LLa/Yb–HLa/Yb boundary (t is negative for LLa/Yb compositions and positive for HLa/Yb), and d corresponds to the K_2O enrichment measured from the primitive trend. In brief, rocks belonging to the same suite have similar t values whereas rocks with identical d values have similar degrees of differentiation.

Sr and Ti contents are also considered in this classification (Fig. 4B). LLa/Yb compositions with $Sr \geq 800$ ppm are termed high-Sr (LLa/Yb-HSr): most of these LLa/Yb-HSr compositions correspond mainly to post-caldera rocks from Santa Maria (Monzier et al., in prep.) and to a few Tanna and Efate rocks. High-Ti (HTi) compositions ($TiO_2 \geq 1\%$) are emphasized, irrespective of their La/Yb character (however, all but two HTi analyses are LLa/Yb and these two only have a very weak HLa/Yb character). Most of the HTi compositions correspond to rocks from Aoba and a few to rocks from Ureparapara, Ambrym, Efate and Vulcan and Eastern Gemini seamounts. Finally, High-Mg andesites (HMA) from the southernmost part of the NHCC are compositionally distinctive, but clearly HLa/Yb in this classification.

4.3. Summarized geochemistry of the whole magmatic suites

Since the main purpose of this paper is to understand the variation of the primary compositions along the NHCC, major- and trace-element behaviour for the entire arc suites will be summarized, using only selected diagrams.

Almost all HLa/Yb composition rocks are from Santa Maria and Aoba volcanoes, the latter being exceptional in this arc for its paucity of differenciated products (Fig. 4A). Only a few rocks from Ambrym, Epi and Kuwae plot in the HLa/Yb field, and interestingly, their HLa/Yb character is quite weak. All rocks from Vanua Lava, Emae, Efate, Erromango, Tanna, Anatom, most of the rocks from Ambrym, Epi and Kuwae, most of the IAB rocks (i.e., belonging to 'normal' Island-Arc Basalt suite;

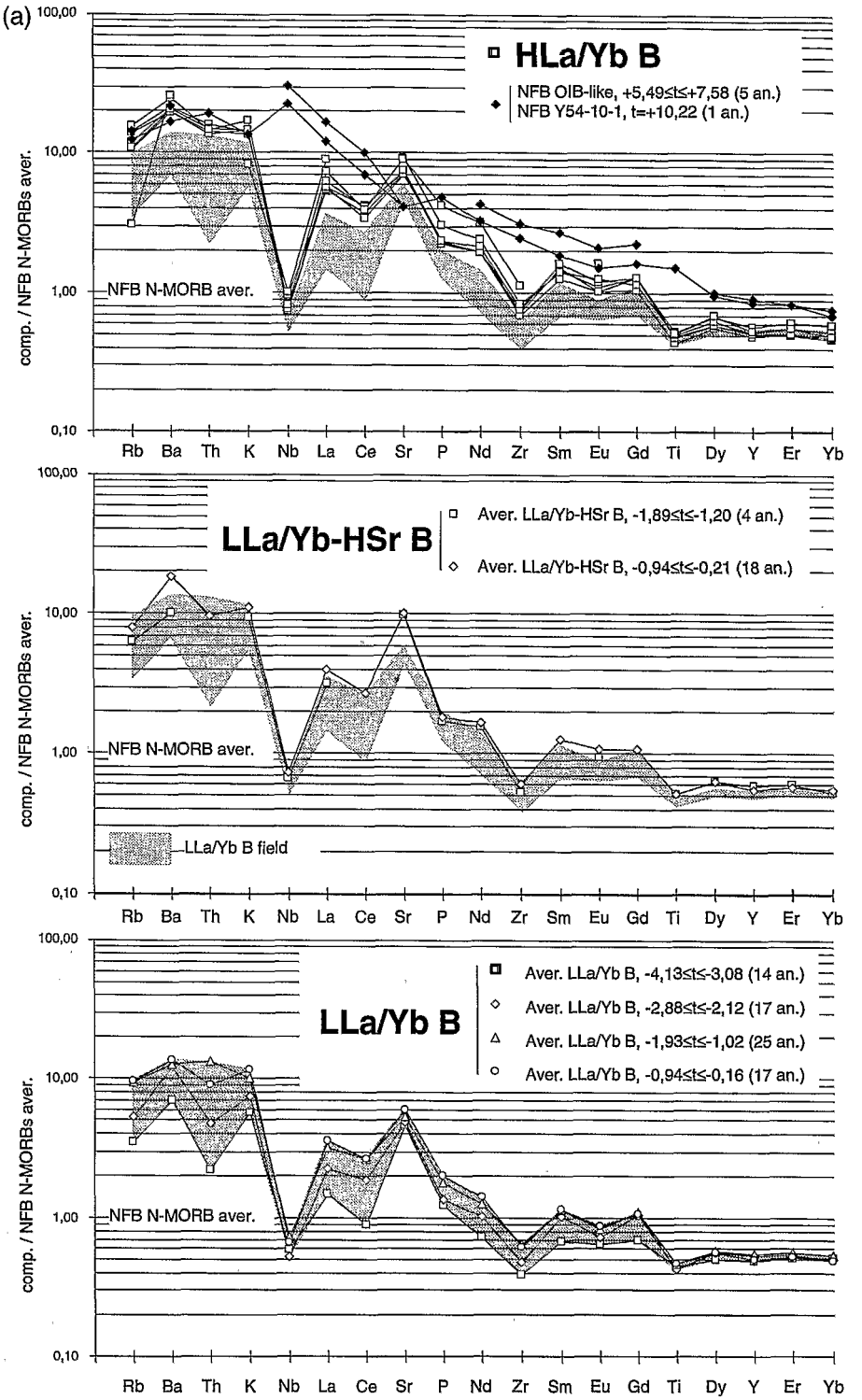
(a)
HLa/Yb B
NFB OIB-like, +5,49≤t≤+7,58 (5 an.)
NFB Y54-10-1, t=+10,22 (1 an.)
NFB N-MORB aver.
LLa/Yb-HSr B
Aver. LLa/Yb-HSr B, -1,89≤t≤-1,20 (4 an.)
Aver. LLa/Yb-HSr B, -0,94≤t≤-0,21 (18 an.)
LLa/Yb B field
LLa/Yb B
Aver. LLa/Yb B, -4,13≤t≤-3,08 (14 an.)
Aver. LLa/Yb B, -2,88≤t≤-2,12 (17 an.)
Aver. LLa/Yb B, -1,93≤t≤-1,02 (25 an.)
Aver. LLa/Yb B, -0,94≤t≤-0,16 (17 an.)
comp. / NFB N-MORBs aver.
100,00
10,00
1,00
0,10
Rb Ba Th K Nb La Ce Sr P Nd Zr Sm Eu Gd Ti Dy Y Er Yb

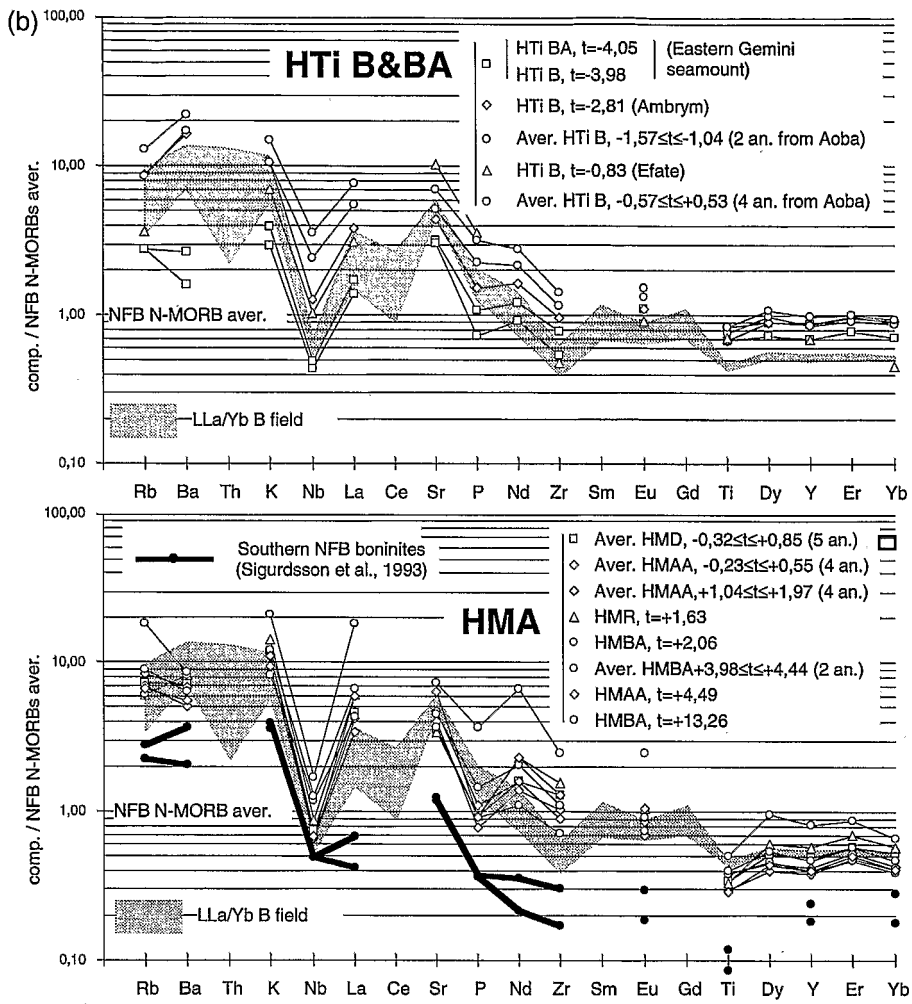

Fig. 6. (a) North Fiji Basin N-MORB normalized incompatible-element abundance patterns for averages of LLa/Yb, LLa/Yb-HSr and HLa/Yb primitive basalts (see Table 1Table 2). The average of 19 N-MORB compositions with low La/Yb values from the N–S axis of the North Fiji Basin has been used for the normalization; normalized patterns for OIB-like basalts with high La/Yb values from the N160°E axis of the North Fiji Basin are shown for HLa/Yb basalts (Eissen et al., 1994; Nohara et al., 1994; Table 1Table 2). (b) North Fiji Basin N-MORB normalized incompatible-element abundance patterns for selected averages of HTi and HMA primitive compositions (see Table 1Table 2). Normalized patterns for southern North Fiji Basin boninites (Sigurdsson et al., 1993) are shown for HMA. *B* = basalt; *BA* = basic andesite; *AA* = acid andesite; *D* = dacite; *HM* = high-magnesium.

Monzier et al., 1993) from the southern submarine end of the SVS, and a few rocks from Santa Maria and Aoba are LLa/Yb (i.e., 'normal').

The SiO_2 vs. Al_2O_3 diagram (Fig. 5a) reveals a linear, negative correlation for most LLA/Yb compositions, starting from high-Al basalts (17–19% Al_2O_3). LLa/Yb-HSr basalts are also distinctly high-Al. In contrast, a general positive correlation is observed for HLa/Yb compositions with < 54% SiO_2, from low-Al (8–9% Al_2O_3) basaltic compositions to high-Al (16–19%) basaltic andesite compositions. HMA are generally slightly depleted in Al_2O_3 when compared to other rocks with similar SiO_2 contents. The same broad linear negative correlations characterize the LLa/Yb and HLa/Yb compositions on the SiO_2 vs. $Fe_2O_3^*$ and CaO diagrams (not shown). Nonetheless, HLa/Yb andesitic compositions are slightly depleted in these elements, com-

Table 1
Average compositions and individual analyses for the 194 'primitive' compositions of the NHCC. Compositions of North Fiji Basin basalts are given for comparison

	LOI	Initial total	wt.% (total recalculated to 100% LOI free)									
			SiO_2	TiO_2	Al_2O_3	$Fe_2O_3^*$	MnO	MgO	CaO	Na_2O	K_2O	P_2O_5
NHCC rocks with $d < 1\%$ K_2O												
LLa/Yb B, $-4.13 \leq t \leq 3.08$ (14 an.) [a]	0.64	100.04	49.69	0.69	18.06	11.21	0.19	5.78	11.40	2.33	0.51	0.14
Standard deviation	0.65	0.49	1.39	0.10	1.06	0.63	0.01	1.38	1.05	0.35	0.22	0.04
LLa/Yb D, $t = -3.24$ [b]	0.30	99.88	66.28	0.57	15.18	6.00	0.14	1.58	4.96	4.07	1.02	0.20
LLa/Yb B, $-2.88 \leq t \leq 2.12$ (17 an.) [a]	0.25	100.03	49.50	0.66	16.51	11.14	0.19	7.13	11.84	2.21	0.67	0.15
Standard deviation	0.50	0.42	1.65	0.13	1.90	0.75	0.02	2.50	1.29	0.53	0.24	0.05
LLa/Yb BA, $-2.61 \leq t \leq -2.39$ (5 an.) [a]	0.67	99.97	54.80	0.73	17.55	10.12	0.19	3.44	8.37	3.29	1.25	0.27
Standard deviation	0.77	0.20	0.84	0.12	1.70	1.66	0.05	0.49	0.25	0.27	0.08	0.05
LLa/Yb D, $t = -2.97$ [b]	0.40	99.89	63.43	0.64	15.50	7.30	0.15	2.11	5.82	3.77	1.09	0.20
LLa/Yb B, $-1.93 \leq t \leq -1.02$ (25 an.) [a]	0.53	100.28	49.83	0.73	16.57	11.44	0.19	6.64	11.09	2.40	0.90	0.20
Standard deviation	0.93	0.48	1.42	0.08	1.79	0.85	0.02	2.37	1.08	0.52	0.29	0.06
LLa/Yb BA, $t = -1.94$ [b]	−0.26	100.00	54.56	0.87	15.91	11.37	0.23	3.69	8.35	3.42	1.31	0.30
LLa/YB B, $-0.94 \leq t \leq -0.16$ (17 an.) [a]	0.19	99.91	49.26	0.72	16.35	11.50	0.20	6.78	11.51	2.42	1.05	0.22
Standard deviation	0.68	0.32	1.21	0.06	2.12	0.66	0.01	2.30	0.76	0.23	0.25	0.04
LLa/Yb-HSr B, $-1.89 \leq t \leq -1.20$ (4 an.) [a]	−0.10	100.21	48.46	0.79	18.52	11.93	0.21	5.56	11.02	2.47	0.85	0.19
Standard deviation	0.49	0.27	0.63	0.02	0.63	0.30	0.01	0.48	0.45	0.07	0.15	0.01
LLa/Yb-HSr B, $-0.94 \leq t \leq -0.21$ (18 an.) [a]	0.27	100.06	50.28	0.80	18.42	10.96	0.22	4.63	10.72	2.78	0.99	0.20
Standard deviation	0.37	0.30	1.23	0.06	0.47	0.41	0.02	0.84	0.71	0.28	0.15	0.06
HLa/Yb B, $+0.12 \leq t \leq +0.99$ (14 an.) [a]	0.03	99.99	49.56	0.82	15.42	11.32	0.20	7.56	11.02	2.62	1.22	0.25
Standard deviation	0.44	0.52	1.19	0.09	2.02	0.57	0.02	3.47	0.67	0.49	0.33	0.05
HLa/Yb BA, $t = 0.80$ [b]	0.33	99.89.	54.14	0.65	18.70	9.88	0.16	3.11	9.88	2.63	0.66	0.15
HLa/Yb B, $+1.12 \leq t \leq +1.97$ (18 an.) [a]	0.45	99.86	49.11	0.77	14.26	11.31	0.20	9.12	11.27	2.43	1.28	0.25
Standard deviation	0.83	0.33	0.78	0.07	1.39	0.45	0.03	2.37	0.78	0.24	0.20	0.03
HLa/Yb B, $+2.00 \leq t \leq +2.99$ (17 an.) [a]	0.19	100.24	48.67	0.68	12.80	11.25	0.19	12.17	10.53	2.14	1.32	0.26
Standard deviation	0.47	0.37	1.30	0.13	2.84	0.66	0.01	5.57	1.05	0.60	0.30	0.05
HLa/Yb BA, $t = 2.05$ [b]	−0.10	100.72	54.85	0.89	15.97	11.06	0.23	3.53	8.25	3.37	1.55	0.30
HLa/Yb B, $+3.05 \leq t \leq +3.76$ (7 an.) [a]	0.64	100.19	48.70	0.74	13.13	11.95	0.21	10.36	11.24	2.10	1.31	0.26
Standard deviation	0.86	0.24	0.74	0.08	2.11	0.36	0.01	4.05	1.18	0.43	0.30	0.04
HLa/Yb BA, $t = 3.70$ [b]	0.43	100.20	54.83	0.82	16.65	11.64	0.19	3.27	8.54	2.84	0.98	0.25

Table 1 (continued)

	LOI	Initial total	wt.% (total recalculated to 100% LOI free)									
			SiO_2	TiO_2	Al_2O_3	$Fe_2O_3^*$	MnO	MgO	CaO	Na_2O	K_2O	P_2O_5
NHCC rocks with d < 1% K_2O												
HLa/Yb B, $+4.23 \le t \le +5.05$ (5 an.) [a]	0.70	99.43	48.47	0.78	13.70	11.99	0.22	8.85	11.52	2.58	1.56	0.33
Standard deviation	0.81	1.86	1.64	0.14	2.64	0.77	0.04	5.07	0.79	0.72	0.27	0.04
HLa/Yb B, $t = 7.39$ [b]	1.96	100.41	49.06	0.80	13.34	12.07	0.21	8.53	12.39	2.39	0.74	0.47
HTi BA, $t = -4.05$ [b]	−0.42	99.79	54.09	1.31	14.90	12.80	0.22	4.35	8.68	3.18	0.35	0.12
HTi B, $t = -3.98$ [b]	−0.29	99.48	52.22	1.05	16.21	11.94	0.21	5.07	10.27	2.69	0.26	0.08
HTi B, $t = -2.81$ [b]	0.93		51.86	1.06	16.56	12.84	0.23	4.09	9.03	3.21	0.96	0.17
HTi B, $-1.57 \le t \le -1.04$ (2 an.) [a]	0.68	99.37	49.59	1.19	14.91	11.98	0.22	7.61	10.92	2.39	0.94	0.25
Standard deviation	0.89	0.33	1.81	0.12	1.06	0.13	0.01	2.04	1.44	0.37	0.19	0.05
HTi B, $t = -0.83$ [b]	0.76	100.29	47.50	1.12	17.63	13.13	0.22	5.28	11.23	2.85	0.63	0.39
HTi B, $-0.57 \le t \le +0.53$ (4 an.) [a]	0.12	100.04	48.60	1.29	15.94	12.08	0.21	6.25	11.31	2.63	1.33	0.35
Standard deviation	0.29	0.22	0.60	0.20	1.01	0.79	0.01	1.44	0.74	0.38	0.13	0.06
HMD, $-0.32 \le t \le +0.85$ (5 an.) [a]	0.72	99.37	63.79	0.53	14.93	6.30	0.10	3.24	6.01	3.99	1.01	0.10
Standard deviation	0.44	0.51	0.62	0.10	0.57	0.48	0.01	0.54	0.37	0.28	0.05	0.03
HMAA, $-0.23 \le t \le +0.55$ (4 an.) [a]	0.27	99.37	62.00	0.46	15.41	6.10	0.10	4.55	6.61	3.67	1.01	0.09
Standard deviation	0.23	0.32	0.68	0.04	0.43	0.04	0.00	1.00	0.16	0.18	0.15	0.01
HMAA, $+1.04 \le t \le +1.97$ (4 an.) [a]	0.24	99.73	59.54	0.60	15.54	7.25	0.12	4.85	7.69	3.43	0.85	0.12
Standard deviation	0.17	0.21	1.76	0.07	0.63	0.79	0.01	0.55	0.81	0.15	0.13	0.03
HMR, $t = +1.63$ [b]	2.45	99.26	69.21	0.52	14.35	4.24	0.09	1.17	3.22	5.82	1.29	0.10
HMBA, $t = +2.06$ [b]	0.45	99.39	54.88	0.59	14.19	8.43	0.15	8.72	9.60	2.60	0.74	0.10
HMBA, $+3.98 \le t \le +4.44$ (2 an.) [a]	0.47	99.94	55.52	0.62	13.80	8.38	0.15	8.65	8.87	2.76	1.09	0.16
Standard deviation	0.03	0.50	0.23	0.04	0.15	0.24	0.00	0.12	0.90	0.22	0.16	0.04
HMAA, $t = +4.49$ [b]	0.08	99.59	61.80	0.45	15.16	6.33	0.11	4.47	6.91	3.66	0.99	0.10
HMB, $t = +13.26$ [b]	0.42	99.06	55.05	0.78	14.02	8.52	0.14	7.83	8.13	3.21	1.92	0.41
NFB rocks for comparison (Eissen et al., 1994; Nohara et al., 1994)												
NFB N-MORB [c], $-4.74 \le t \le -4.32$ (19 an.)	−0.60	99.76	49.76	1.55	14.45	11.80	0.18	7.65	11.97	2.43	0.09	0.11
NFB OIB-like B [d], $+5.49 \le t \le +7.58$ (5 an.)	1.87	100.27	49.42	2.34	16.38	9.03	0.16	7.86	9.97	3.10	1.22	0.53
NFB Y54-10-1 B [e], $t = 10.22$												

B = basalt; BA = basic andesite; AA = acid andesite; D = dacite; HM = high-magnesium.

[a] Average or [b] single composition.

[c] Average of 19 N-MORB compositions with low La/Yb values from the N–S axis of the NFB (Nohara et al., 1994).

[d] Average of 5 OIB-like basalts with high La/Yb values from the N160°E axis of the NFB (Nohara et al., 1994).

[e] Y54-10-1, OIB-like basalt with the highest La/Yb value from the N160°E axis of the NFB (Nohara et al., 1994).

Table 2
Average compositions and individual analyses for the 194 'primitive' compositions of the NHCC. Compositions of North Fiji Basin basalts are given for comparison

	ppm																				
	Sc	V	Cr	Co	Ni	Rb	Sr	Y	Zr	Nb	Ba	La	Ce	Nd	Sm	Eu	Gd	Dy	Er	Yb	Th
NHCC rocks with $d < 1\%$ K_2O																					
LLa/Yb B, $-4.13 \leq t \leq 3.08$ (14 an.)[a]	37	334	64	35	28	6	433	16.4	30	1.2	130	3.2	6.3	5.9	1.7	0.71	2.03	2.48	1.62	1.58	0.28
Standard deviation	6	44	56	6	14	3	74	2.8	7	0.7	43	0.8	0.9	1.1	0.2	0.11	0.17	0.49	0.41	0.27	0.15
LLa/Yb D, $t = -3.24$[b]	19	75	2	6	2	16	340	29.0	69	1.0	138	7.2		12.0		1.20		4.60	2.80	2.85	
LLa/Yb B, $-2.88 \leq t \leq 2.12$ (17 an.)[a]	40	340	181	39	51	9	456	17.7	36	1.1	229	4.9	13.2	8.5	2.6	0.80	3.07	2.83	1.72	1.54	0.62
Standard deviation	10	39	217	5	43	4	135	4.0	14	0.4	138	1.4	1.4	2.2	0.2	0.20	0.29	0.52	0.38	0.34	0.06
LLa/Yb BA, $-2.61 \leq t \leq -2.39$ (5 an.)[a]	25	221	11	30	10	21	421	22.8	68	2.1	349	8.2		12.6		1.05		4.05	2.75	2.39	
Standard deviation	6	55	4	6	3	4	108	2.0	8	0.3	53	1.1		0.4		0.16		0.21	0.23	0.29	
LLa/Yb D, $t = -2.97$[b]	21	125	2	11	2	17	386	27.0	66	0.8	124	7.2		13.5		1.05		4.30	2.90	2.55	
LLa/Yb B, $-1.93 \leq t \leq -1.02$ (25 an.)[a]	37	339	156	41	57	17	489	18.1	50	1.5	241	7.0	18.9	10.4	3.0	0.90	3.23	2.90	1.80	1.65	1.71
Standard deviation	7	54	181	6	54	10	110	3.5	13	0.7	86	1.5	4.5	2.1	0.5	0.16	0.46	0.50	0.36	0.31	1.62
LLa/Yb BA, $t = -1.94$[b]	30	248	14	30	12	16	400	27.5	79	2.3	412	10.4		15.0		1.40		4.50	2.90	2.60	
LLa/YB B, $-0.94 \leq t \leq -0.16$ (17 an.)[a]	35	331	180	42	62	17	555	16.5	47	1.3	258	7.8	19.0	11.7	3.0	0.94	3.14	2.82	1.67	1.49	1.17
Standard deviation	5	39	186	6	51	6	62	1.4	12	0.5	54	1.0	2.2	1.8	0.3	0.10	0.31	0.24	0.18	0.20	0.24
LLa/Yb-HSr B, $-1.89 \leq t \leq -1.20$ (4 an.)[a]	30	356	34	37	27	11	932	19.5	40	1.4	189	6.9		12.7		1.01		3.13	1.93	1.63	
Standard deviation	4	27	7	2	3	3	28	2.1	3	0.6	18	0.9		1.2		0.13		0.17	0.19	0.14	
LLa/Yb-HSr B, $-0.94 \leq t \leq -0.21$ (18 an.)[a]	25	436	18	34	16	14	940	18.4	46	1.5	345	8.6	19.0	13.5	3.2	1.17	3.20	3.16	1.84	1.67	1.27
Standard deviation	3	26	46	4	18	3	46	2.1	6	0.4	38	1.2	1.4	1.5	0.4	0.16	0.49	0.31	0.23	0.24	0.17
HLa/Yb B, $+0.12 \leq t \leq +0.99$ (14 an.)[a]	33	360	196	37	86	19	663	19.3	61	1.9	372	11.8	26.6	16.1	3.8	1.18	3.84	3.36	1.97	1.80	1.84
Standard deviation	5	31	237	7	83	5	130	3.1	14	0.9	104	2.5	5.7	3.0	0.6	0.22	0.51	0.55	0.34	0.32	0.44

HLa/Yb BA, $t = 0.80$ [b]	28	320	17	22	13	9	562	16.1	41	1.1	110	10.2		14.0		0.95		2.60	1.90	1.60	
HLa/Yb B, $+1.12 \leq t \leq +1.97$ (18 an.) [a]	34	352	288	43	127	21	688	17.3	56	1.5	395	12.2	29.5	16.2	4.0	1.10	3.80	2.93	1.77	1.62	2.08
Standard deviation	2	29	164	7	68	3	84	1.8	6	0.3	64	1.3	3.5	1.7	0.3	0.17	0.30	0.31	0.23	0.16	0.07
HLa/Yb B, $+2.00 \leq t \leq +2.99$ (17 an.) [a]	32	302	463	51	220	25	656	16.1	53	1.5	373	12.3	24.2	16.1	3.3	1.12	3.08	2.83	1.62	1.47	1.78
Standard deviation	5	60	358	15	163	9	157	3.0	12	0.4	95	2.8	4.0	3.4	0.5	0.22	0.50	0.54	0.36	0.32	0.21
HLa/Yb BA, $t = 2.05$ [b]	30	245	15	31	13	24	398	31.0	139	5.1	420	23.5		27.5		1.25		5.00	3.50	2.90	
HLa/Yb B, $+3.05 \leq t \leq +3.76$ (7 an.) [a]	36	330	333	53	154	19	694	16.9	58	1.6	390	13.4	29.0	17.7	4.2	1.30	3.83	2.92	1.60	1.43	1.95
Standard deviation	5	48	232	9	121	7	121	2.8	10	0.4	95	2.3	5.1	2.5	0.4	0.19	0.34	0.40	0.22	0.22	0.47
HLa/Yb BA, $t = 3.70$ [b]	31	350	10	26	10	13	643	20.0	63	1.6	167	17.0		21.0		1.35		3.00	2.30	1.80	
HLa/Yb B, $+4.23 \leq t \leq +5.05$ (5 an.) [a]	34	336	245	47	102	28	854	16.9	64	1.7	470	15.7	28.0	20.0	3.6	1.37	3.38	3.16	1.64	1.47	1.90
Standard deviation	4	68	330	12	134	11	172	2.7	10	0.4	100	2.8	5.0	3.3	0.6	0.19	0.42	0.69	0.26	0.25	0.50
HLa/Yb B, $t = 7.39$ [b]	38	335	305	45	80	6	840	18.0	87	2.1	483	19.5		26.0		1.75		3.50	1.80	1.50	
HTi BA, $t = -4.05$ [b]	42	460	4	28	9	5	295	29.0	60	1.0	30	3.7		10.0		1.20		4.50	3.10	2.75	
HTi B, $t = -3.98$ [b]	42	330	30	30	15	5	284	23.0	41	0.9	50	3.0		7.5		0.95		3.60	2.50	2.20	
HTi B, $t = -2.81$ [b]						16	416	29.0	73	2.6	310	8.3		13.4		1.18		4.44	3.05	2.84	
HTi B, $-1.57 \leq t \leq -1.04$ (2 an.) [a]	38	361	195	33	74	16	479	28.0	88	5.0	320	12.0		17.6		1.42		4.88	2.94	2.69	
Standard deviation	6	6	114	0	29	5	9	4.0	18	0.5	26	2.5		2.4		0.13		0.42	0.36	0.34	
HTi B, $t = -0.83$ [b]	28	474	31	43	17	7	972	23.1	37	2.1		6.7				1.00				1.42	
HTi B, $-0.57 \leq t \leq +0.53$ (4 an.) [a]	37	427	107	31	49	23	645	32.1	108	7.3	412	16.6		22.9		1.66		5.34	3.17	2.87	
Standard deviation	3	54	99	0	23	6	23	3.5	22	3.0	15	2.3		3.0		0.25		0.80	0.48	0.35	
HMD, $-0.32 \leq t \leq +0.85$ (5 an.) [a]	22	163	51	14	17	13	338	16.3	100	1.5	133	9.9		13.1		0.91		2.54	1.84	1.62	
Standard deviation	1	10	25	1	6	2	34	3.4	18	0.3	26	1.9		2.0		0.14		0.48	0.36	0.27	

Table 2 (continued)

	ppm																			
	Sc	V	Cr	Co	Ni	Rb	Sr	Y	Zr	Nb	Ba	La	Ce	Nd	Sm	Eu	Gd	Dy	Er	Yb	Th
NHCC rocks with d < 1% K_2O																					
HMAA, $-0.23 \leq t \leq +0.55$ (4 an.) [a]	22	158	124	18	55	15	371	12.5	78	1.3	127	7.4		11.4		0.75		1.98	1.54	1.25	
Standard deviation	1	11	74	3	36	5	49	0.4	6	0.1	44	0.5		0.8		0.11		0.11	0.14	0.04	
HMAA, $+1.04 \leq t \leq +1.97$ (4 an.) [a]	29	221	127	19	39	13	445	13.7	68	1.4	95	9.2		13.1		0.93		2.25	1.68	1.30	
Standard deviation	3	60	41	3	7	3	71	2.2	12	0.2	6	1.2		2.8		0.13		0.53	0.29	0.21	
HMR, $t = +1.63$ [b]	13	50	2	3	5	11	320	19.0	119	1.8	155	13.2		19.0		1.15		3.00	2.20	1.75	
HMBA, $t = +2.06$ [b]	33	235	339	33	128	11	345	13.3	54	2.4	153	9.2		9.0		0.80		2.30	1.50	1.20	
HMBA, $+3.98 \leq t \leq +4.44$ (2 an.) [a]	31	245	327	32	152	16	418	15.6	84	2.6	121	14.3		17.0		1.00		2.70	1.85	1.43	
Standard deviation	3	15	21	2	34	3	14	2.4	27	0.6	5	1.7		6.0		0.25		0.40	0.35	0.13	
HMAA, $t = +4.49$ [b]	23	150	94	18	30	12	597	13.3	99	1.4	103	12.8		19.0		1.15		2.20	1.60	1.25	
HMB, $t = +13.26$ [b]	28	270	260	25	93	33	684	27.0	188	3.5	161	40.0		55.0		2.70		4.80	2.80	2.05	
NFB rocks for comparison (Eissen et al., 1994; Nohara et al., 1994)																					
NFB N-MORB [c], $-4.74 \leq t \leq -4.32$ (19 an.)	42	300	261	43	86	2	93	33.0	76	2.1	19	2.2	7.1	8.2	2.6	1.08	2.94	4.98	3.17	3.06	0.13
NFB OIB-like B [d], $+5.49 \leq t \leq +7.58$ (5 an.)	30	297	291	33	142	22	383	28.2	188	46.1	314	26.3	49.9	26.6	4.9	1.63	4.77	4.80	2.63	2.13	2.50
NFB Y54-10-1 B [e], $t = 10.22$						25	381	30.0	237	62.8	408	35.9	71.9	35.6	7.0	2.25	6.61	5.03	2.64	2.33	

[a] Average or [b] single composition.
[c] Average of 19 N-MORB compositions with low La/Yb values from the N–S axis of the NFB (Nohara et al., 1994).
[d] Average of 5 OIB-like basalts with high La/Yb values from the N160°E axis of the NFB (Nohara et al., 1994) .
[e] Y54-10-1, OIB-like basalt with the highest La/Yb value from the N160°E axis of the NFB (Nohara et al., 1994).

pared to the LLa/Yb compositions. Most HMA compositions are $Fe_2O_3^*$ (and TiO_2 and MnO) depleted and CaO enriched. The SiO_2 vs. MgO diagram (Fig. 5a) reveals a linear, negative correlation for most LLA/Yb compositions. A general negative correlation is also observed for HLa/Yb compositions, with accumulation of olivine and clinopyroxene certainly responsible for the sharp bend occurring near 50% SiO_2 and the trend towards high-MgO (and low-Al_2O_3) contents. Obviously, HMA are distinctly Mg-rich.

The SiO_2 vs. Na_2O and K_2O (Fig. 5b) diagrams show two broad positive trends, LLa/Yb compositions being depleted in these elements compared to HLa/Yb compositions. As previously noted, some LLa/Yb compositions from Ambrym have an anomalous high-K (or low-Si) character. In addition, HMA compositions are strongly depleted in K (and, to a lesser extent, in Na).

Relationships between Ba and SiO_2 contents (Fig. 5b), as well as relationships between Rb, Nb, Zr, La and SiO_2 contents (not shown), are quite similar to those displayed in the SiO_2 vs. K_2O diagram, with two distinct LLa/Yb and HLa/Yb linear positive trends converging towards basaltic compositions, and a flat and significantly depleted HMA trend. The MgO vs. Sr diagram (Fig. 5a) also clearly discriminates the LLa/Yb and HLa/Yb compositions and, obviously, the post-caldera LLa/Yb-HSr basalts from Santa Maria. Finally, both the LLa/Yb and the HLa/Yb compositions delineate the same broad positive trend on the Y and Yb vs. SiO_2 diagrams (not shown); all HTi compositions plot above this trend whereas HMA compositions display a flat and distinctly depleted trend.

4.4. Geochemistry of the primitive compositions

A selection of 194 'primitive' compositions with $d \leq 1$ (grey field on Fig. 4A–B), including 79 LLa/Yb, 22 LLa/Yb-HSr, 64 HLa/Yb, 10 HTi and 19 HMA, has been used to draw up the Tables 1 and 2. Each class is subdivided into subclasses using t parameter values (as shown in Fig. 4A). Obviously, true primitive basalts as well as slightly differenciated basalts are included in this selection; however, in a statistical approach to obtain a representative view of the entire NHCC, all of these compositions have been incorporated in the average calculations for 'primitive' basalts. Additionally, twelve basic andesites and dacites with a 'primitive' character (i.e., with an unusually low K_2O content), and HMA, have been considered separately for calculations.

The four calculated averages for the LLa/Yb basalts (Tables 1 and 2) show very similar SiO_2, TiO_2, $Fe_2O_3^*$, MnO, CaO, Na_2O, Sc, V, HREE and Y contents. As expected, they show increasing K_2O, P_2O_5, LILE, LREE and Zr contents with increasing t values. However, the average for the compositions with $t \leq -3.8$ have higher Al_2O_3 (18% vs. 16.5%) and lower MgO (6% vs. 7%), Cr, Ni and Co than the three other LLa/Yb averages. The two calculated averages for the LLa/Yb-HSr basalts are quite similar to those calculated for other LLa/Yb basaltic compositions, except for the Al_2O_3, Sr and Na_2O contents which are higher.

The low-Al and high-Mg (and high-Cr and -Ni) character of the HLa/Yb basalts is clearly indicated by the five average compositions, when compared with the LLa/Yb compositions. In addition, these HLa/Yb compositions have slightly lower SiO_2 contents, slightly higher TiO_2 and MnO contents, and clearly higher K_2O, P_2O_5, LILE, LREE and Zr contents than the corresponding LLa/Yb compositions, but comparable $Fe_2O_3^*$, CaO and Na_2O contents.

The average of nineteen N-MORB compositions with low La/Yb values from the N–S-oriented axis of the North Fiji Basin (Tables 1 and 2; Eissen et al., 1994; Nohara et al., 1994) has been used for the normalization of incompatible elements. The NFB-MORB-normalized incompatible-element abundance patterns for the LLa/Yb averages (Fig. 6a) show typical arc-lava features, with relative (but variable) enrichment of LILE and LREE compared to HFSE and HREE, a negative Nb anomaly, a strong positive Sr anomaly, and HFSE and HREE levels below the NFB-MORB level. For the LLa/Yb basic andesite and dacite compositions with 'primitive' character, the NFB-MORB-normalized incompatible-element abundance patterns (not shown) remain, in a general way, just above those of the LLa/Yb basalts; however, they show unusually high HREE and Y levels, comparable to those of the NFB-MORB. The NFB-MORB-normalized patterns for the LLa/Yb-HSr basalts coincide with the most enriched LLa/Yb

basaltic compositions (Fig. 6a), except for a strong positive Sr anomaly which is not accompanied by a positive Eu anomaly.

The NFB-MORB-normalized incompatible-element abundance patterns for the HLa/Yb averages are almost perfectly parallel and plot above the LLa/Yb patterns (Fig. 6a), except for the HREE which are quite similar for both groups. Typical arc-lava features, including the strong negative Nb anomaly, a positive Sr anomaly and levels of HFSE and HREE well below NFB-MORB levels, are obvious. For comparison, normalized patterns for OIB-like basalts with high La/Yb values from the N160°E axis of the NFB (Eissen et al., 1994; Nohara et al., 1994) are given. These patterns show a progressive increase in incompatible-element contents from Yb to Nb and plot well above the HLa/Yb basaltic compositions (but most of the HLa/Yb compositions are significantly more mafic than these NFB OIB-like basalts; Tables 1 and 2). Considering only the REE and Y contents, the patterns for both OIB-like basalts from the North Fiji Basin and HLa/Yb basalts are almost parallel; however, the LILE contents (Sr excluded) are quite similar for the two groups. The three HLa/Yb basic andesite compositions (Tables 1 and 2) have quite variable characteristics, but one of them, from Ambrym, has HREE contents similar to those of the NFB-MORB compositions, whereas the other two have more usual low-HREE levels (diagrams not shown).

Average and individual compositions for HTi basalts and basic andesites show variable characteristics apart from their high-Ti contents (Tables 1 and 2). NFB-MORB-normalized incompatible-element abundance patterns (Fig. 6b) confirm this wide compositional spectrum. Nevertheless, Ti, HREE and Y contents are always above those of other NHCC basalts, i.e., slightly below the NFB-MORB level, and the negative Nb anomaly is weak. In addition, as noted by Monzier et al. (1993), the REE and Y contents for the two basic andesites from Eastern Gemini Seamount do not differ markedly from those of the NFB-MORB.

Calculated compositions or individual analyses for HMA are given in Tables 1 and 2. Corresponding NFB-MORB-normalized incompatible-element abundance patterns (Fig. 6b) are quite similar to those of the LLa/Yb basaltic compositions, but with a notably higher Zr content, higher contents of K, Nb, La, Nd, comparable contents of Rb, Sr and Eu and lower contents of Ba, P, Ti and HREE. One composition from Vauban seamount ($t = +13.26$) differs from the other HMA compositions by a strong enrichment in all incompatible elements (see Monzier et al., 1993). Lastly, it is apparent that the HMA compositional trends broadly parallel the southern North Fiji Basin boninites trend (Sigurdsson et al., 1993).

5. Discussion

5.1. Volcano distribution

Based on the best constrained sections shown in Fig. 3, large volcanoes are generally 170–220 km above the slab, this distance decreasing to 80–90 km for the HMAVS small edifices (not shown in Fig. 3; see Monzier et al., 1984b, 1993). At Erromango, beneath which the slab is continuous (Fig. 3J), recent volcanism appears well anchored just above an intermediate seismic swarm. This swarm probably corresponds to a zone of intense reactions within the slab, leading to the melting of the overlying mantle. Nevertheless, in Fig. 3A–D, the dense swarms of intermediate seismicity and the volcanoes (Vanua Lava, Santa Maria, Aoba and Ambrym) are not located on the same vertical line. This discrepancy could be explained if, according to Spiegelman and McKenzie (1987), the fluids (or melt phases) released from the slab are not driven by buoyant percolation alone, but rather tend to be drawn toward the hotter core of the mantle wedge (i.e., the principal site of magma generation; Eggins, 1989, 1993). Another explanation would be the lateral displacement of the sinking pieces of the slab in relation to the volcanoes. Such an explanation may be proposed for Ambrym and Vanua Lava, where slab detachment is obvious, but is probably not applicable for Aoba and Santa Maria, where the slab is barely (or not?) broken.

5.2. Compositional changes of the primitive compositions along the NHCC

Primitive compositions ($d \leq 1$) are considered for the study of the geochemical variations along the

NHCC. To avoid data gaps, the file is completed with a few major-element analyses of Ureparapara, Lopevi and Vulcan basalts, for which REE data is not available. Considering their locations, these rocks are probably LLa/Yb, i.e., 'normal'.

Variations of La/Yb along the NHCC are shown in Fig. 7. On this diagram, the LLa/Yb rocks clearly define the 'normal' trend of the NH arc whereas the HLa/Yb rocks delineate two strong anomalies, one in front of the DEZ collision zone and one corresponding to the HMAVS (plus a few rocks from the neighbouring Volsmar seamount). In the DEZ collision zone, compositions from Santa Maria and Aoba form the anomaly peak with very high La/Yb. Interestingly, the upper limit of this anomaly is distinctly asymmetric, with a sharp northward decrease between Santa Maria and Vanua Lava and a progressive southward decrease from Aoba to Kuwae. Note that the corresponding lower limit of the LLa/Yb field also shows a similar asymmetric pattern.

The SiO_2% along-arc variation diagram (Fig. 8A) displays minimum values for Santa Maria and Aoba, where basalts with 45–47% SiO_2 are common, and a progressive SiO_2 enrichment from Tanna to the southern HMA. The only two dacites with 'primitive' character in our data file come from the southern end of the SVS (Western Gemini seamount; see discussion of these particular rocks in Monzier et al., 1993). The Na_2O% variation pattern is similar to that of SiO_2 (Fig. 8F). The Al_2O_3% variation pattern is strikingly spoon-shapped (Fig. 8C), with predominant low-Al compositions at Aoba and Santa Maria (nevertheless, the post caldera LLa/Yb-HSr basalts from Santa Maria are clearly Al-rich), both low- and high-Al rocks at Ambrym, predominant high-Al rocks at Ureparapara, Vanua Lava and from Lopevi to Erromango, and a continuous decrease in Al_2O_3% from Erromango to the southern HMA. The K_2O content pattern is exactly the opposite (Fig. 8G), with unusually high-K basalts at Aoba and Santa Maria and a continuous increase in K_2O from Erromango to the HMA. P_2O_5% variation (not shown) is quite similar to that of K_2O, but with a broader scattering and no constant enrichment from Erromango to the HMA (in contrast, the HMA are depleted in P_2O_5 compared to the Anatom–Gemini–Volsmar rocks). For the CVS, the MgO% variation pattern (Fig. 8E) parallels that of K_2O%; basalts with a high MgO content (i.e., > 10%) are frequent

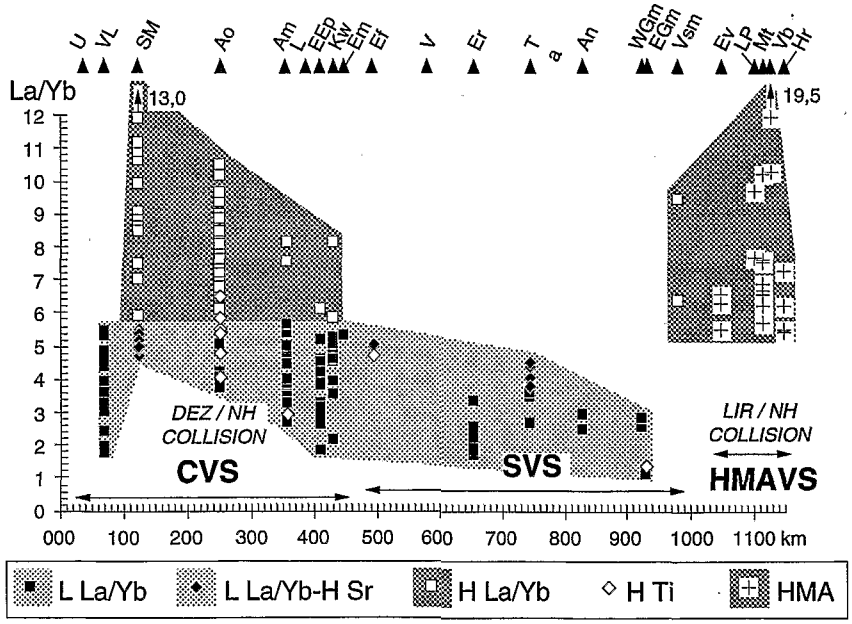

Fig. 7. Variation of the La/Yb ratio along the New Hebrides Central Chain (only primitive compositions are reported; see Fig. 4); volcano names as in Fig. 2.

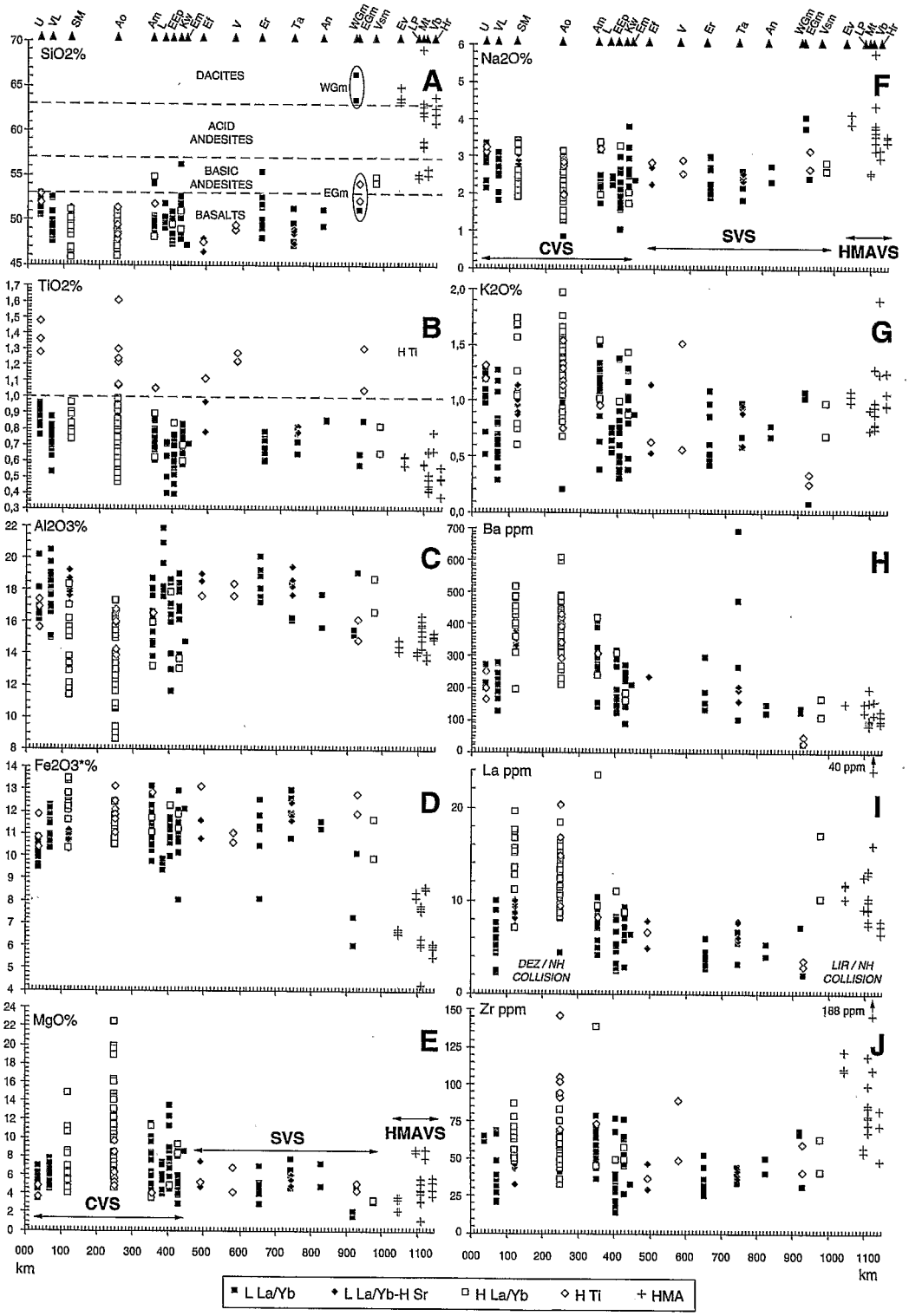
SiO2%
DACITES
ACID ANDESITES
BASIC ANDESITES
BASALTS
WGm
EGm
A
TiO2%
H Ti
B
Al2O3%
C
Fe2O3*%
D
MgO%
E
CVS
SVS
HMAVS
Na2O%
F
K2O%
G
Ba ppm
H
La ppm
40 ppm
DEZ / NH COLLISION
LIR / NH COLLISION
I
Zr ppm
188 ppm
J
km
L La/Yb
L La/Yb-H Sr
H La/Yb
H Ti
HMA

at Aoba and, to a lesser extent, at Santa Maria, Ambrym and Epi. All other rocks are normal in terms of MgO content, with the exception of the most primitive HMA, which contain 8.5–8.8% MgO. In spite of some scatter, Fe_2O_3 (Fig. 8D), MnO and CaO (not shown) contents show little variation all along the NHCC, except for the southern termination where they fall abruptly in the HMA. The TiO2% variation (Fig. 8B) is not systematic, with HTi rocks present in several volcanoes along the arc. Apparently, TiO_2% strongly increases between Lopevi and Vulcan seamount, whereas it remains quite constant from Erromango to Western Gemini seamount. As for Fe_2O_3, this content falls at the southern extremity of the NHCC.

The Cr, Co and Ni content variations along the NHCC (not shown) closely reflect those of MgO, with high values (Cr > 300 ppm, Ni > 100 ppm) frequent for Aoba rocks and less frequent for Santa Maria, Ambrym and Epi rocks. The most primitive HMA from the southern termination of the NHCC also present high contents in these compatible elements (306 < Cr < 347 ppm, 118 < Ni < 185 ppm). Lastly, the Sc content along-arc pattern (not shown) is quite unclear, but displays a continuous decrease from Erromango rocks to the southern HMA.

Among the LILE (Rb, Ba and Sr), the most striking behaviour is that of the Ba content (Fig. 8H), which shows a definite peak for Santa Maria and Aoba rocks and, to a lesser extent, Ambrym rocks, and low values for all other rocks, including those from the southern HMA. Note the sharp decrease in Ba content between Santa Maria and Vanua Lava rocks whereas the decrease from Ambrym to Kuwae is more gradual. The Rb content pattern along the NHCC is very similar to that of K_2O. A broad scattering affects the Sr content, but a peak is obvious for Santa Maria and Aoba. The La (LREE) and Zr (HFSE) content patterns (Fig. 8I,J) reflect, with much less scatter, that of K_2O. The Yb (HREE) and Y contents remain quite constant all along the NHCC (diagrams not shown), with high values only for the HTi samples and a weak decrease from the SVS rocks to the HMA.

Thus, in front of the DEZ collision zone, a general increase in La/Yb occurs, with Santa Maria and Aoba rocks displaying the highest values. Major-element variations along the arc clearly illustrate: (1) the anomalous, Mg- and K-rich, Al- and Si-poor, character of the rocks from Aoba and Santa Maria (and, to a lesser extent, from Ambrym); this anomaly, recognized since Gorton (1974, 1977), may be partly explained, with the exception of the K enrichment, by olivine accumulation in these rocks; (2) the existence of a compositional transition between the 'normal' rocks of the SVS and the HMA of the southern termination of the NHCC. Trace-element variations along the arc are in good agreement with major-element variations, especially the strong enrichments in Rb, Ba, Sr, Zr and La, which parallel the K enrichment at Aoba and Santa Maria.

5.3. Model of magma generation

The peculiar compositions of the rocks from the volcanoes facing the DEZ have always been related, more or less directly, to the DEZ collision–subduction. The DEZ subduction probably provokes a modification of the mantle thermal regime in the source region of the arc magmas, leading to lower degrees of partial melting and the generation of high-K magmatic suites. Nevertheless, Briqueu et al. (1994) demonstrated isotopically that the DUPAL-type mantle source of these anomalous high-K products is the result of a long-term (> 500 m.y.) enrichment process. More recently, Crawford et al. (1995) explained the unusual characteristics of these volcanoes by an eastward (50–100 km) and downward deflection of the site of arc magmatism in front of the collision zone, such that dehydratation of the slab leads to magma generation, not from the usual Pacific-type MORB mantle source in the mantle wedge present under all other volcanoes of the NHCC, but from an Indian Ocean-type MORB mantle source,

Fig. 8. Variation of selected major and trace elements along the New Hebrides Central Chain (only primitive compositions are reported; see Fig. 4); volcano names as in Fig. 2.

presently ascending under both the embryonic New Hebrides backarc troughs and the volcanoes facing the DEZ.

The DEZ collision began at approximately 3 Ma at the latitude of Epi island and the impact zone has experienced a northward migration since that time (Greene and Collot, 1994). Therefore, a direct relationship between the DEZ subduction and the geochemistry of the NHCC should show a concomitant northward migration of the geochemical anomaly, followed by a progressive return to 'normal' magmatic arc processes on its trailing edge. As a consequence, HLa/Yb rocks covered by LLa/Yb rocks should be expected to occur from Kuwae to Ambrym, whereas in Aoba (presently in front of the DEZ), recent lavas would be only of the HLa/Yb type. Our detailed sampling allows us to discuss these topics.

— South of Kuwae, only LLa/Yb compositions exist along the SVS of the NHCC, and at Epi island and Kuwae LLa/Yb compositions predominate during the entire evolution of these volcanoes.

— On Ambrym, HLa/Yb basalts are scarce and do not correspond to recent products. The few differentiated rocks with a weak HLa/Yb character come from both the basal shield volcano and the recent (< 2000 yr B.P.) post-caldera suite (MacCall et al., 1970; Robin et al., 1993; Picard et al., 1995). In contrast, almost all basalts and differentiated rocks are LLa/Yb, independent of their stratigraphical position. At this mostly subaerial volcano (according to the bathymetric map of Chase and Seekins, 1988), our detailed sampling (Picard et al., 1995) is certainly sufficient to definitively preclude the existence of a HLa/Yb inner core capped by post-collision LLa/Yb products. Thus, this volcano appears largely dominated by LLa/Yb magmatism.

— Scarce, old Ti-rich lavas from Aoba island (Eggins, 1993) may be, on the basis of trace-element data, related to pre-DEZ collision Pliocene (3.65–3.30 Ma) sills, sampled in the North Aoba Basin at ODP Hole 833 (Hasenaka et al., 1994). These rocks, which have lower La/Yb than the young lavas from Aoba island, might correspond to a pre-DEZ collision volcanic phase (note that the voluminous submarine edifice has not been sampled), even if pre-collision 'normal' rocks are not usually Ti-rich. Most samples from Aoba island are young HLa/Yb basalts, but a few recent LLa/Yb (but not HTi) basalts also occur. As these scarce LLa/Yb rocks are overlain by HLa/Yb formations, they cannot mark a progressive reversion to 'normal' post-collision compositions.

Thus, the relationship, in terms of leading edge and wake effects, between the LILE and LREE enrichment and the northward migration of the DEZ collision zone is not tenable. This is confirmed by the anomaly peak which clearly coincides with Santa Maria, an area probably still unaffected by the DEZ subduction. On this well sampled island, all pre-caldera basalts and differentiated rocks are HLa/Yb, which implies that 'normal' LLa/Yb pre-caldera suites probably never occurred, given the mostly subaerial nature of the volcano (according to the bathymetric map of Chase and Seekins, 1988). Moreover, all recent (post-caldera) basalts are LLa/Yb (even if this LLa/Yb character is relatively weak; Figs. 4 and 7). These recent basalts are also unusually Sr-rich (and also Al_2O_3- and Na_2O-rich) for 'normal' LLa/Yb basalts, possibly as a consequence of plagioclase phenocryst accumulation in a shallow magmatic chamber (Monzier et al., in prep.). Thus, a few thousands of years ago, a marked change from HLa/Yb lavas to LLa/Yb lavas occurred at Santa Maria, apparently without a concomitant tectonic change. As post-caldera lavas are only basaltic, they probably correspond to the ascent of a new magma batch following the complete emptying of an earlier magma chamber. North of Santa Maria, at Vanua Lava island, only LLa/Yb compositions exist, a remarkable feature given the small distance between the two islands.

Therefore, rather than an interpretation related to the DEZ subduction and its northward migration along the arc, an alternative interpretation based on a strong geochemical anomaly located under Santa Maria and Aoba islands is preferred. As no fractional crystallization process can link LLa/Yb and HLa/Yb primitive compositions, this geochemical anomaly is linked to discrete mantle source compositions. Moreover, as shown by isotopic data, it cannot have a slab origin (Briqueu et al., 1994). In contrast, isotopic data suggest that a DUPAL-type mantle, result of a long-term (> 500 m.y.) enrichment process, is the probable source of the HLa/Yb products (Briqueu et al., 1994).

Normal arc magma generation occurs by melting in the mantle wedge of a residual upper mantle source previously depleted by BABB melt extraction and driven by convection in the mantle wedge (Woodhead et al., 1993). We suggest that an E–W-oriented strip of enriched mantle under the N160°E axis of the North Fiji Basin may extend westward beneath Santa Maria and Aoba islands, and may well explain both the generation of enriched 'OIB-like' basalts along this axis (Eissen et al., 1994; Nohara et al., 1994) and the generation of the HLa/Yb anomalous magmas of the NHCC. Given the few compositions with a weak HLa/Yb character found at Ambrym, Epi and Kuwae, and the continuous spectrum existing from LLa/Yb to HLa/Yb compositions (Fig. 4), some limited participation of the enriched source in the magma generation should occur in the mantle wedge under this volcanic segment. Conversely, some limited participation of the depleted source in the magma generation under Santa Maria and Aoba is also likely.

If the ascent of enriched mantle under the Santa Maria–Aoba volcanoes (and the backarc troughs) is occurring, in contrast, the proposed eastward deflection of the site of arc magmatism (Crawford et al., 1995) is really not evident for the Santa Maria–Aoba segment, where the peak anomaly is located (Fig. 2). Such a deflection clearly exists for the Ambrym–Kuwae segment, but the geochemical anomaly in this zone is weak. Thus, the interpretation by Crawford et al. (1995), which correlates the unusual characteristics of the DEZ volcanoes to an eastward and downward deflection of the site of arc magmatism in front of the collision zone, is not supported by our data and model.

In conclusion, since ≈ 3–2 Ma, a westward and upward invasion of enriched mantle, well sustained by the distribution of the intermediate seismicity (200–259 km deep) under the central part of the arc (Fig. 9) seems to better explain the anomalous geochemistry of volcanics from Santa Maria and Aoba. The unusual longitudinal distribution of the intermediate seismicity beneath Santa Maria and Aoba, with the top of a seismic arch overlying an aseismic core, strongly supports the ascent of such an enriched mantle diapir (Figs. 2 and 3). Furthermore, ascent of this diapir would also explain the peculiar arched form of the detached slab beneath Ureparapara to Efate. The detachment, probably triggered by the collision of the DEZ with the arc, would be less important under the Santa Maria–Aoba segment than under Ureparapara–Vanua Lava and Ambrym–Efate segments, because of the upward motion of the mantle diapir beneath Santa Maria and Aoba, which

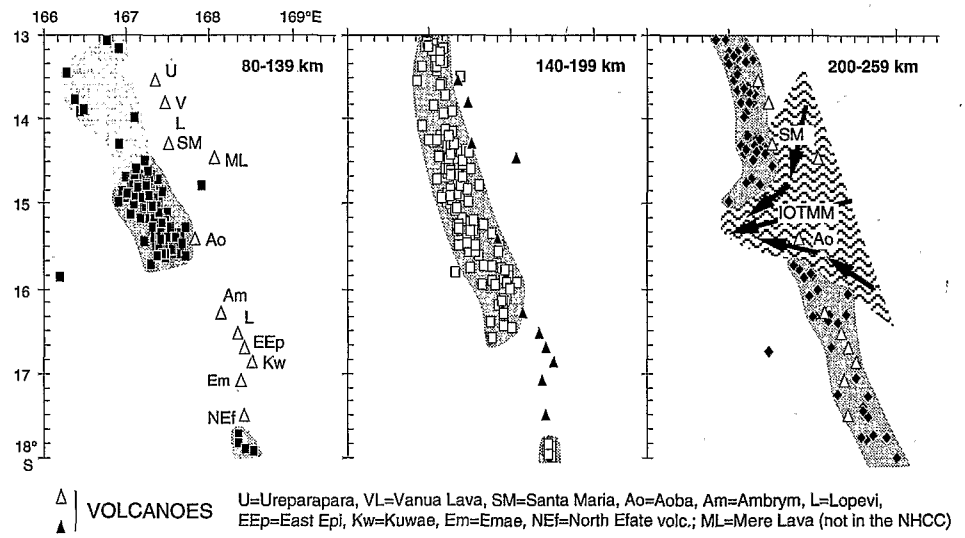

Fig. 9. Intermediate seismicity (USGS–NEIC, 1961–1988; $n > 20$ stations) under the central part of the New Hebrides arc. The slab is outlined and the westward and upward propagation of a deep regional body of Indian Ocean-type MORB mantle (*IOTMM*) beneath Santa Maria and Aoba islands is represented (see text and Fig. 2Fig. 3).

would support and slow down the sinking slab. The westward and upward invasion of upper mantle considered here obviously contrasts with the general convective motion established under the arc (Fig. 3), which would likely enhance mechanical and chemical mixing between depleted and enriched material. This would account for the variable participation of both sources in magma generation in the central part of the arc.

The very recent change in the characteristics of Santa Maria volcanism (post-caldera LLa/Yb-HSr basalts) probably corresponds to a move towards a more 'typical' situation, with magmas being issued from a more 'normal' depleted mantle (Fig. 2). This emphasizes (i) either the instability of the anomaly (due to variations in the mechanical and chemical mixing between enriched and depleted mantle?) or a modification in the deep feeding circuit as shown in Fig. 2, and (ii) the close connection between deep and crustal-level evolution in arc magmatism.

Finally, from Tanna to Hunter volcanoes, the existence of a compositional transition between the rocks of the SVS and the HMAVS implies a decreasing participation of the 'normal' depleted mantle source, combined with a greater participation of the high-Ca boninites refractory source in NHCC magmatism. The complex history of this southern termination of the arc, with evolving transform plate motions related to both the intersection between the N–S-oriented North Fiji Basin spreading axis and the arc, and the Loyalty Ridge collision, probably favoured this progressive interplay between the two magmatic sources.

Acknowledgements

We thank A.J. Crawford and I.E. Smith for constructive reviews that substantially improved the manuscript. This work is part of a research program, developed at the Department of Geology, Mines and Water Resources in Vanuatu, and supported by ORSTOM UR 14 and French Foreign Affairs Ministry (MAE). The entire geochemical data base (Microsoft Excel 4.0) on which this paper is founded is available on request (M.M.).

References

Ash, R.P., Carney, J.N. and Macfarlane, A., 1978. Geology of Efate and offshore islands. Reg. Rep., New Hebrides Condominium Geol. Surv., Port Vila, New Hebrides, 55 pp.

Ash, R.P., Carney, J.N. and Macfarlane, A., 1980. Geology of the northern Banks islands. Reg. Rep., New Hebrides Gov. Geol. Surv., Port Vila, New Hebrides, 58 pp.

Auzende, J.-M., Pelletier, B. and Lafoy, Y., 1994. Twin active spreading ridges in the North Fiji Basin (southwest Pacific). Geology, 22: 63–66.

Barsdell, M. and Berry, R.F., 1990. Origin and evolution of primitive island arc ankaramites from western Epi, Vanuatu. J. Petrol., 31(3): 747–777.

Barsdell, M., Smith, I.E.M. and Spörli, K.B., 1982. The origin of reversed geochemical zoning in the northern New Hebrides volcanic arc. Contrib. Mineral. Petrol., 81: 148–155.

Blot, C., 1972. Volcanisme et séismes du manteau supérieur dans l'archipel des Nouvelles-Hébrides. Bull. Volcanol., 36(3): 446–461.

Briqueu, L., Laporte, C., Crawford, A.J., Baker, P.E. and Coltorti, M., 1994. Temporal magmatic evolution of the Aoba Basin, central New Hebrides island arc: Pb, Sr, and Nd isotopic evidence for the coexistence of two mantle component beneath the arc. Proc. ODP, Sci. Results, 134: 393–401.

Burne, R.V., Collot, J.-Y. and Daniel, J., 1988. Superficial structures and stress regimes of the downgoing plate associated with subduction–colllision in the central New Hebrides arc (Vanuatu). In H.G. Greene et F.L. Wong (Editors), Geology and Offshore Resources of Pacific Island Arcs — Vanuatu Region. Circum-Pac. Counc. Energy Miner. Resour., Earth Sci. Ser., 8: 357–376.

Calmant, S., Lebellegard, P., Taylor, F., Bevis, M., Maillard, D., Recy, J. and Bonneau, J., 1995. Geodetic measurements of convergence across the New Hebrides subduction zone. Geophys. Res. Lett., 22(19): 2573–2576.

Carney, J.N. and Macfarlane, A., 1979. Geology of Tanna, Aneytyum, Futuna and Aniwa. Reg. Rep., New Hebrides Gov. Geol. Surv., Port Vila, New Hebrides, 79 pp.

Charvis, Ph. and Pelletier, B., 1989. The northern New Hebrides back-arc troughs: history and relation with the North Fiji Basin. Tectonophysics, 170: 259–277.

Chase, T.E. and Seekins, B.A., 1988. Submarine topography of the Vanuatu and southeastern Solomon islands regions. In: H.G. Greene and F.L. Wong (Editors), Geology and Offshore Resources of Pacific Islands Arcs — Vanuatu Region. Circum-Pac. Counc. Energy Miner. Resour., Earth Sci. Ser., 8: 35.

Chatelain, J.-L., Molnar, P., Prévot, R. and Isacks, B., 1992. Detachment of part of the downgoing slab and uplift of the New Hebrides (Vanuatu) islands. Geophys. Res. Lett., 19(14): 1507–1510.

Chatelain, J.-L., Guillier, B. and Gratier, J.-P., 1993. Unfolding the subducting plate in the central New Hebrides island arc: geometrical argument for detachment of part of the downgoing slab. Geophys. Res. Lett., 20(8): 655–658.

Colley, H. and Ash, R.P., 1971. The geology of Erromango. Reg. Rep., New Hebrides Condominium Geol. Surv., Port Vila, New Hebrides, 124 pp.

Collot, J.-Y. and Fisher, M.A., 1989. Formation of forearc basins by collision between seamounts and accretionary wedges: an example from the New Hebrides subduction zone. Geology, 17: 930–933.

Collot, J.-Y., Daniel, J. and Burne, R.V., 1985. Recent tectonics associated with the subduction/collision of the d'Entrecasteaux Zone in the central New Hebrides. Tectonophysics, 112: 325–356.

Collot, J.-Y., Lallemand, S., Pelletier, B., Eissen, J.-P., Glaçon, G., Fisher, M.A., Greene, H.G., Boulin, J., Daniel, J. and Monzier, M., 1992. Geology of the d'Entrecasteaux–New Hebrides Arc collision zone: results from a deep submersible survey. Tectonophysics, 212: 213–241.

Coudert, E., Cardwell, R.K., Isacks, B.L. and Chatelain, J.-L., 1984. P-wave velocity of the uppermost mantle and crustal thickness in the central Vanuatu islands (New Hebrides island arc). Bull. Seismol. Soc. Am., 74(3): 913–924.

Coulon, C. and Maury, R.C., 1981. Petrology of tholeiitic lavas from Tanna island (New Hebrides): importance of cumulatives processes in island arc magmatism. Bull. Volcanol., 44(4): 661–680.

Coulon, C., Maillet, P. and Maury, R.C., 1979. Contribution à l'étude du volcanisme de l'arc des Nouvelles-Hébrides: données pétrologiques sur les laves de l'île d'Efaté. Bull. Soc. Géol. Fr., 7, XXI(5): 619–629.

Crawford, A.J., Greene, H.G. and Exon, N.F., 1988. Geology, petrology and geochemistry of submarine volcanoes around Epi island, New Hebrides island arc. In: H.G. Greene and F.L. Wong (Editors), Geology and Offshore Resources of Pacific Islands Arcs — Vanuatu Region. Circum-Pac. Counc. Energy Miner. Resour., Earth Sci. Ser., 8: 301–327.

Crawford, A.J., Falloon, T.J. and Green, D.H., 1989. Classification, petrogenesis and tectonic setting of boninites. In: A.J. Crawford (Editor), Boninites. Unwin Hyman, London, pp. 1–49.

Crawford, A.J., Danyushevsky, L., Sigurdsson, I., Monzier, M. and Eggins, S.M., 1993. Tectonic controls on magmatism in the southern New Hebrides (Vanuatu) island arc. IAVCEI General Assembly, Canberra, 1993, p. 24 (abstract).

Crawford, A.J., Briqueu, L., Laporte, C. and Hasenaka, T., 1995. Coexistence of Indian and Pacific oceanic upper mantle reservoirs beneath the central New Hebrides island arc. In: Active Margins and Marginal Basins of the Western Pacific. Am. Geophys. Union, Geophys. Monogr., 88: 199–217.

Dupuy, C., Dostal, J., Marcelot, G., Bougault, H., Joron, J.L. and Treuil, M., 1982. Geochemistry of basalts from central and southern New Hebrides arc: implication for their source rock composition. Earth Planet. Sci. Lett., 60: 207–225.

Eggins, S.M., 1989. The origin of primitive ocean island and island arc basalts. Ph.D. Thesis, Univ. Tasmania, 402 pp. (unpubl.).

Eggins, S., 1993. Origin and differentiation of picritic arc magmas, Ambae (Aoba), Vanuatu. Contrib. Mineral. Petrol., 114: 79–100.

Eissen, J.-P., Nohara, M., Cotten, J. and Hirose, K., 1994. North Fiji Basin basalts and their magma sources: Part I. Incompatible elements constraints. Mar. Geol., 116: 153–178.

Gill, J.B., 1981. Orogenic Andesites and Plate Tectonics. Springer, Berlin, 390 pp.

Girod, M., Maury, R.C. and Barsdell, M., 1979. Coexistence de basaltes sursaturés et sous-saturés en silice aux Nouvelles-Hébrides: problème de leurs relations génétiques, C. R. Acad. Sci. Paris, D, 288: 1355–1358.

Gorton, M.P., 1974. The geochemistry and geochronology of the New Hebrides. Ph.D. Thesis, Australian Natl. Univ., 300 pp.

Gorton, M.P., 1977. The geochemistry and origin of Quaternary volcanism in the New Hebrides. Geochim. Cosmochim. Acta, 41: 1257–1270.

Greene, H.G. and Collot, J.-Y., 1994. Ridge-arc collision: timing and deformation determined by Leg 134 drilling, central New Hebrides island arc. Proc. ODP, Sci. Results, 134: 609–621.

Greene, H.G., Macfarlane, A., Johnson, D.P. and Crawford, A.J., 1988. Structure and tectonics of the central New Hebrides arc. In: H.G. Greene et F.L. Wong (Editors), Geology and Offshore Resources of Pacific Island Arcs — Vanuatu Region. Circum-Pac. Counc. Energy Miner. Resour., Earth Sci. Ser., 8: 377–412.

Greene, H.G., Collot, J.-Y., Fisher, M.A. and Crawford, A.J., 1994. Neogene tectonic evolution of the New Hebrides island arc: a review incorporating ODP drilling results. Proc. ODP, Sci. Results, 134: 19–46.

Hasenaka, T., Crawford, A.J., Briqueu, L., Coltorti, M., Baker, P.E. and Fujinawa, A., 1994. Magmatic evolution of the north Aoba intra-arc basin: sites 832 and 833. Proc. ODP, Sci. Results, 134: 375–392.

Ibrahim, A.K., Pontoise, B., Latham, G., Larue, M., Chen, T., Isacks, B., Recy, J. and Louat, R., 1980. Structure of the New Hebrides arc–trench system. J. Geophys. Res., 85(B1): 253–266.

Louat, R. and Pelletier, B., 1989. Seismotectonics and present-day relative plate motions in the New Hebrides–North Fiji Basin region. Tectonophysics, 167: 41–55.

Louat, R., Hamburger, M. and Monzier, M., 1988. Shallow and intermediate-depth seismicity in the New Hebrides arc: constraints on the subduction process. In: H.G. Greene et F.L. Wong (Editors), Geology and Offshore Resources of Pacific Island Arcs — Vanuatu Region. Circum-Pac. Counc. Energy Miner. Resour., Earth Sci. Ser., 8: 329–356.

MacCall, G.J.H., LeMaitre, R.W., Malahoff, A., Robinson, G.P. and Stephenson, P.J., 1970. The geology and geophysics of the Ambrym caldera, New Hebrides. Bull. Volcanol., 34: 681–696.

Macfarlane, A., Carney, J.N., Crawford, A.J. and Greene, H.G., 1988. Vanuatu — A review of the onshore geology. In: H.G. Greene et F.L. Wong (Editors), Geology and Offshore Resources of Pacific Island Arcs — Vanuatu Region. Circum-Pac. Counc. Energy Miner. Resour., Earth Sci. Ser., 8: 45–91.

Maillet, P., Monzier, M., Selo, M. and Storzer, D., 1983. The d'Entrecasteaux Zone (Southwest Pacific). A petrological and geochronological reappraisal. Mar. Geol., 53: 179–197.

Maillet, P., Monzier, M. and Lefèvre, C., 1986. Petrology of

Matthew and Hunter volcanoes, south New Hebrides island arc (Southwest Pacific).J. Volcanol. Geotherm. Res., 30: 1–27.

Mallick, D.I.J. and Ash, R.P., 1975. Geology of the southern Banks islands. Reg. Rep., New Hebrides Condominium Geol. Surv., Port Vila, New Hebrides, 39 pp.

Marcelot, G., 1980. Contribution à l'étude du volcanisme des Nouvelles-Hébrides: pétrographie, minéralogie et géochimie des laves d'Erromango. Thèse 3ème Cycle, Univ. Paris-Sud, Centre d'Orsay, 273 pp.

Marcelot, G., 1981. Géochimie des laves de l'ile Erromango (Nouvelles-Hébrides): implications pétrogénétiques, Bull. Soc. Géol. Fr., 7, XXIII(4): 367–376.

Marcelot, G., Maury, R.C. and Lefevre, C., 1983. Mineralogy of Erromango lavas (New Hebrides): evidence of an early stage of fractionation in island arc basalts. Lithos, 16: 135–151.

Marthelot, J.-M., Chatelain, J.-L., Isacks, B.L., Cardwell, R.K. and Coudert, E., 1985. Seismicity and attenuation in the central Vanuatu (New Hebrides) islands: a new interpretation of the effect of subduction of the d'Entrecasteaux fracture zone. J. Geophys. Res., 90(B10): 8641–8650.

Mitropoulos, P. and Tarney, J., 1992. Significance of mineral composition variations in the Aegean Island Arc. J. Volcanol. Geotherm. Res., 51: 283–303.

Monjaret, M.-C., 1989. Le magmatisme des fossés à l'arrière de l'arc des Nouvelles-Hébrides (Vanuatu). Thèse Doct., Univ. Bretagne Occidentale, Brest, 516 pp.

Monzier, M., 1993. Un modèle de collision arc insulaire–ride océanique. Evolution sismo-tectonique et pétrologie des volcanites de la zone d'affrontement 'Arc des Nouvelles-Hébrides–Ride des Loyauté'. Thèse Doct., Univ. 'Sciences de la Terre', Univ. Française du Pacifique, Nouméa, New Caledonia, 322 pp.

Monzier, M., Collot, J.Y. and Daniel, J., 1984a. Carte bathymétrique des parties centrale et méridionale de l'arc insulaire des Nouvelles-Hébrides. Map at 1/1.036.358. ORSTOM, Paris.

Monzier, M., Maillet, P., Foyo Herrera, J., Louat, R., Missegue, F. and Pontoise, B., 1984b. The termination of the Southern New Hebrides subduction zone (southwestern Pacific). Tectonophysics, 101: 177–184.

Monzier, M., Daniel, J. and Maillet, P., 1990. La collision 'ride des Loyauté/arc des Nouvelles-Hébrides' (Pacifique Sud-Ouest). Oceanol. Acta, Vol. Spéc., 10: 43–56.

Monzier, M., Maillet, P. and Dupont, J., 1992. Carte bathymétrique des parties méridionales de l'arc insulaire des Nouvelles-Hébrides et du bassin Nord-Fidjien. Map at 1/1.036.358. Inst. Fr. Rech. Sci. Dév. Coop., 'ORSTOM, Paris.

Monzier, M., Danyushevsky, L.V., Crawford, A.J., Bellon, H. and Cotten, J., 1993. High-Mg andesites from the southern termination of the New Hebrides island arc (SW Pacific). J. Volcanol. Geotherm. Res., 57: 193–217.

Monzier, M., Robin, C. and Eissen, J.-P., 1994. Kuwae (≈ 1425 A.D.): the forgotten caldera. J. Volcanol. Geotherm. Res., 59: 207–218.

Nohara, M., Hirose, K., Eissen, J.-P., Urabe, T. and Joshima, M., 1994. The North Fiji Basin basalts and their magma sources: Part II. Sr-Nd isotopic and trace element constraints. Mar. Geol., 116: 179–195.

Pelletier, B., Lafoy, Y. and Missègue, F., 1993. Morphostructure and magnetic fabric of the northwestern North Fiji Basin. Geophys. Res. Lett., 20(12): 1151–1154.

Picard, C., Monzier, M., Eissen, J.-P. and Robin, C., 1995. Concomitant evolution of tectonic environment and magma geochemistry, Ambrym volcano (Vanuatu, New Hebrides arc). In: J.L. Smellie (Editor), Volcanism Associated with Extension at Consuming Plate Margins. Geol. Soc. Am., Spec. Publ., 81: 135–154.

Pontoise, B., Latham, G.V., Daniel, J., Dupont, J. and Ibrahim, A.B., 1980. Seismic refraction studies in the New Hebrides and Tonga area. UN ESCAP, CCOP/SOPAC Tech. Bull., 3: 47–58.

Pontoise, B., Charvis, Ph. and Gérard, M., 1994. Sedimentary and crustal structure of the North Aoba Basin from seismic refraction data. Proc. ODP, Sci. Results, 134: 549–563.

Prévot, R., Chatelain, J.-L., Roecker, S.W. and Grasso, J.-R., 1994. A shallow double seismic zone beneath the central New Hebrides (Vanuatu): evidence for fragmentation and accretion of the descending plate?. Geophys. Res. Lett., 21(19): 2159–2162.

Recy, J., Pelletier, B., Charvis, Ph., Gérard, M., Monjaret, M.-C. and Maillet, P., 1990. Structure, âge et origine des fossés arrière-arc des Nouvelles-Hébrides. Oceanol. Acta, Vol. Spéc., 10: 43–60.

Robin, C., Eissen, J.-P. and Monzier, M., 1993. Giant tuff cone and 12 km-wide associated caldera at Ambrym Volcano (Vanuatu, New Hebrides Arc). J. Volcanol. Geotherm. Res., 55: 225–238.

Robin, C., Eissen, J.-P. and Monzier, M., 1994a. Ignimbrites of basaltic andesite and andesite compositions from Tanna, New Hebrides Arc. Bull. Volcanol., 56: 10–22.

Robin, C., Monzier, M. and Eissen, J.-P., 1994b. Formation of the mid-fifteenth century Kuwae caldera (Vanuatu) by an initial hydroclastic and subsequent ignimbritic eruption. Bull. Volcanol., 56: 170–183.

Robin, C., Eissen, J.-P. and Monzier, M., 1995. Mafic pyroclastic flows at Santa Maria (Gaua) volcano, Vanuatu: the caldera formation problem in mainly mafic island arc volcanoes. Terra Nova, 7: 436–443.

Roca, J.-L., 1978. Contribution à l'étude pétrologique et structurale des Nouvelles-Hébrides. Thèse Doct. 3ème Cycle, Univ. Sci. Tech. Languedoc, Montpellier, 157 pp.

Sage, F. and Charvis, Ph., 1991. Structure profonde de la transition arc insulaire-bassin marginal dans le nord des Nouvelles-Hébrides (Vanuatu, Pacifique sud-ouest). C. R. Acad. Sci. Paris, II, 313: 41–48.

Sigurdsson, I.A., Kamenetsky, V.S., Crawford, A.J., Eggins, S.M. and Zlobin, S.K., 1993. Primitive island arc and oceanic lavas from the Hunter Ridge–Hunter Fracture Zone: evidence from glass, olivine and spinel compositions. Mineral. Petrol., 47: 149–170.

Simkin, T., Siebert, L., McClelland, L., Bridge, D., Newhall, C.

and Latter, J.H., 1981. Volcanoes of the World. Smithson. Inst., Hutchinson Ross, Stroudsburg, PA, 233 pp.

Spiegelman, M. and McKenzie, D., 1987. Simple 2-D models for melt extraction at mid-ocean ridges and island arcs. Earth Planet. Sci. Lett., 83: 137–152.

Taylor, F.W., Quinn, T.M., Gallup, C.G. and Edwards, R.L., 1994. Quaternary plate convergence rates at the New Hebrides island arc from the chronostratigraphy of Bougainville Guyot (Site 831). Proc. ODP, Sci. Results, 134: 47–57.

USGS–NEIC (U.S. Geological Survey–National Earthquake Information Center), 1961–1988. Preliminary Determinations of Epicenters, monthly listing. Denver, CO.

Vallot, J., 1984. Volcanites draguées au large de l'arc insulaire des Nouvelles-Hébrides; implications pétrogénétiques. Thèse 3ème Cycle, Univ. Paris-Sud, Centre d'Orsay, 172 pp.

Warden, A.J., 1967. The geology of the Central Islands, New Hebrides. Geol. Surv., Port Vila, Vanuatu, Rep. 5, 108 pp.

Warden, A.J., 1970. Evolution of Aoba caldera volcano, New Hebrides. Bull. Volcanol., XXXIV(1): 107–140.

Warden, A.J., Curtis, R., Mitchell, A.H.G. and Espirat, J.-J., 1972. Geology of the Central Islands, 1: 100.000. New Hebrides Geol. Surv. Sheet 8, Port Vila, Vanuatu.

Woodhead, J., Eggins, S. and Gamble, J., 1993. High field strength and transition element systematics in island arc and back-arc basin basalts: evidence for multi-phase melt extraction and a depleted mantle wedge. Earth Planet. Sci. Lett., 114: 491–504.

US mailing notice – *Journal of Volcanology and Geothermal Research* (ISSN 0327-0272) is published monthly by Elsevier Science B.V., (Molenwerf 1, Postbus 211, 1000 AE Amsterdam). Annual subscription price in the USA US$ 1630.00 (US$ price valid in North, Central and South America only), including air speed delivery. Periodicals postage rate is paid at Jamaica, NY 11431. USA POSTMASTERS: Send address changes to *Journal of Volcanology and Geothermal Research,* Publications Expediting, Inc., 200 Meacham Avenue, Elmont, NY 11003.
Airfreight and mailing in the USA by Publications Expediting.

Advertising information
Advertising orders and enquiries may be sent to: Elsevier Science, Advertising Department, The Boulevard, Langford Lane, Kidlington, Oxford, OX5 1GB, UK, tel.: (+44) (0) 1865 843565, fax: (+44) (0) 1865 843952. *In the USA and Canada:* Weston Media Associates, attn. Dan Lipner, P.O. Box 1110, Greens Farms, CT 06436-1110, USA, tel.: (203) 261 2500, fax: (203) 261 0101. *In Japan:* Elsevier Science Japan, Marketing Services, 1-9-15 Higashi-Azabu, Minato-ku, Tokyo 106, Japan, tel.: (+81) 5 5561 5033, fax: (+81) 5 5561 5047.

Note to contributors
A detailed *Guide for Authors* is available upon request. Please pay special attention to the following notes:

Language
The official language of the journal is English, but occasional articles in French and German will be considered for publication. Such articles should start with an abstract in English, headed by an English translation of the title. An abstract in the language of the paper should follow the English abstract. English translations of the figure and table captions should also be given.

Preparation of the text
(a) The manuscript should preferably be prepared on a word processor and printed with double spacing and wide margins and include an abstract of not more than 500 words.
(b) Authors should use IUGS terminology. The use of S.I. units is also recommended.
(c) The title page should include the name(s) of the author(s), their affiliations, fax and e-mail numbers. In case of more than one author, please indicate to whom the correspondence should be addressed.

References
(a) References in the text consist of the surname of the author(s), followed by the year of publication in parentheses. All references cited in the text should be given in the reference list and vice versa.
(b) The reference list should be in alphabetical order.

Tables
Tables should be compiled on separate sheets and should be numbered according to their sequence in the text. Tables can also be sent as glossy prints to avoid errors in typesetting.

Illustrations
(a) All illustrations should be numbered consecutively and referred to in the text.
(b) Drawings should be lettered throughout, the size of the lettering being appropriate to that of the drawings, but taking into account the possible need for reduction in size. The page format of the journal should be considered in designing the drawings.
(c) Photographs must be of good quality, printed on glossy paper.
(d) Figure captions should be supplied on a separate sheet.
(e) If contributors wish to have their original figures returned this should be requested in proof stage at the latest.
(f) Colour figures can be accepted providing the reproduction costs are met by the author. Please consult the publisher for further information.

Page proofs
One set of page proofs will be sent to the corresponding author, to be checked for typesetting/editing. The author is not expected to make changes or corrections that constitute departures from the article in its accepted form. To avoid postal delay, authors are requested to return corrections to the desk-editor, Mr. Herman E. Engelen, by FAX (+31-20-4852459) or e-mail (h.engelen@elsevier.nl), preferably within 3 days.

Reprints
Fifty reprints of each article are supplied free of charge. Additional reprints can be ordered on a reprint order form which will be sent to the corresponding author upon receipt of the accepted article by the publisher.

Submission of manuscripts
Manuscripts should be sent directly to one of the editors (in triplicate). Illustrations should also be submitted in triplicate. All illustrative material should be submitted as glossy prints or high-definition laser print-outs. Furthermore, authors are encouraged to submit their final text also in electronic form in order to speed up the publication process after acceptance of their paper (see Submission of electronic text). Authors are requested to give their FAX and e-mail numbers for immediate communication.
Submission of an article is understood to imply that the article is original and unpublished and is not being considered for publication elsewhere.
Upon acceptance of an article by the journal, the author(s) will be asked to transfer the copyright of the article to the publisher. This transfer will ensure the widest possible dissemination of information under the US Copyright Law.
Authors in Japan please note: Upon request, Elsevier Science Japan will provide authors with a list of people who can check and improve the English of their paper (*before submission*). Please contact our Tokyo office: Elsevier Science Japan, 20-12 Yushima 3-chome, Bunkyo-ku, Tokyo 113; Tel. (03)-3833-3821; Fax (03)-3836-3064.

Submission of electronic text
In order to publish the paper as quickly as possible after acceptance, authors are encouraged to submit the final text also on a 3.5" or 5.25" diskette. Both double density (DD) and high density (HD) diskettes are acceptable. Make sure, however, that the diskettes are formatted according to their capacity (HD or DD) before copying the files onto them. Similar to the requirements for manuscript submission, main text, list of references, table and figure legends should be stored in separate text files with clearly identifiable file names. The format of these files depends on the wordprocessor used. Texts made with Display Write, Multimate, Microsoft Word, Samna Word, Sprint, Volkswriter, Wang PC, Word MARC, WordPerfect, Wordstar, or supplied in DCA/RFT, or DEC/DX format can be readily processed. In all other cases the preferred format is DOS text or ASCII. Essential is that the *name and version of the wordprocessing program, type of computer on which the text was prepared, and format of the text files* are clearly indicated. Authors are encouraged to ensure that the *disk version and the hardcopy must be identical.* Discrepancies can lead to proofs of the wrong version being made.

THERE ARE NO PAGE CHARGES